

Spatial and temporal dynamics of coupled groundwater and nitrogen fluxes through a streambed in an agricultural watershed

Casey D. Kennedy,^{1,2} David P. Genereux,² D. Reide Corbett,³ and Helena Mitasova²

Received 26 August 2008; revised 20 January 2009; accepted 24 April 2009; published 3 September 2009.

[1] This paper presents results on the spatiotemporal dynamics of the coupled water flux (v) and nitrogen fluxes ($f_N = v[N]$, where $[N]$ is the concentration of a dissolved N species) through a streambed in an agricultural watershed in North Carolina. Physical and chemical variables were measured at numerous points in the streambed of a 0.26-km reach: hydraulic conductivity (K) and head gradient (J) and the concentrations of NO_3^- and other N species in streambed groundwater, from which water flux ($v = KJ$) and N fluxes (e.g., $f_{\text{NO}_3} = v[\text{NO}_3^-]$) through the streambed were computed, mapped, and integrated in space. The result was a novel set of streambed maps of the linked variables (K , J , v , and N concentrations and fluxes), showing their spatial variability and how it changed over a year (on the basis of seven bimonthly sets of maps). Mean f_{NO_3} during the study year was $154 \text{ mmol m}^{-2} \text{ d}^{-1}$; this NO_3^- flux, together with that of dissolved organic nitrogen ($f_{\text{DON}} = 17 \text{ mmol m}^{-2} \text{ d}^{-1}$), accounted for >99% of the total dissolved N flux through the streambed. Repeat measurements at the same locations on the streambed show significant temporal variability in f_{NO_3} , controlled largely by changes in v rather than changes in $[\text{NO}_3^-]$. One of the clearest and most persistent aspects of spatial variability was lateral variability across the channel from bank to bank. K and v values were greater in the center of the channel; this distribution of K (ultimately a reflection of sediment dynamics in the channel) apparently focuses groundwater discharge toward the center of the channel. The opposite pattern (low values in the center) was found for J , $[\text{NO}_3^-]$, and (to a lesser extent) f_{NO_3} . Overall, f_{NO_3} was characterized by localized zones of high and low values that changed in size and shape over time but remained in basically the same locations (the same was true of K , J , and $[\text{NO}_3^-]$, though less so for v), with 70% of NO_3^- flux occurring through about 38% of the streambed area. Lateral distributions of the physical hydrologic attributes (K , J , and v) were highly symmetrical across the channel, while those of $[\text{NO}_3^-]$ and f_{NO_3} showed higher values on the left than on the right, likely a reflection of different N use on opposite sides of the stream. The streambed-based approach taken here offers insights concerning the spatial and temporal dynamics of linked water and N fluxes through a streambed and their controls.

Citation: Kennedy, C. D., D. P. Genereux, D. R. Corbett, and H. Mitasova (2009), Spatial and temporal dynamics of coupled groundwater and nitrogen fluxes through a streambed in an agricultural watershed, *Water Resour. Res.*, 45, W09401, doi:10.1029/2008WR007397.

1. Introduction

[2] Land application of nitrogen (N) in the form of agricultural fertilizer increased in the U.S. from 0.5 billion kg N a^{-1} in 1945 [Puckett, 1995] to 11.2 billion kg N a^{-1} in 1999 [Howarth et al., 2002], and agriculture affects 70% of rivers and streams with “impaired” water quality [U.S.

Environmental Protection Agency and U.S. Department of Agriculture, 1998]. Transport of N from groundwater to surface water is potentially among the largest N fluxes in the environment, and may become larger as pollution continues and groundwater systems become further “charged” with N, as has already occurred in places [Böhlke and Denver, 1995; Böhlke, 2002; Tesoriero et al., 2007]. Nitrate (NO_3^-) may be the most ubiquitous contaminant of groundwater worldwide [Spalding and Exner, 1993], and when carried into streams and rivers by groundwater discharge may degrade water quality and adversely affect ecosystems [e.g., Boesch et al., 2001; Rabalais et al., 2001]. Groundwater NO_3^- may also be denitrified and the resultant N_2 discharged harmlessly into surface water. Other N species such as ammonium (NH_4^+) may in some cases account for a significant fraction of the total N loading from

¹Department of Earth and Atmospheric Sciences, Purdue University, West Lafayette, Indiana, USA.

²Department of Marine, Earth, and Atmospheric Sciences, North Carolina State University, Raleigh, North Carolina, USA.

³Department of Geological Sciences and Institute of Coastal Science and Policy, East Carolina University, Greenville, North Carolina, USA.

groundwater to surface water [e.g., *Chestnut and McDowell*, 2000]. The work described here addresses the question of how to use field data to quantify N fluxes from groundwater to surface water.

[3] A number of studies have addressed N transport from groundwater to streams or rivers, directly or indirectly, and mostly for NO_3^- . Some have focused on subsurface data collection and analysis in vertical cross sections normal to streams [e.g., *Böhlke and Denver*, 1995; *Tesoriero et al.*, 2000; *Lindsey et al.*, 2003; *Böhlke et al.*, 2002; *Spruill et al.*, 2005; *Tesoriero et al.*, 2005], with an emphasis on the evolution of groundwater age and N chemistry along groundwater flow lines, and the orientation of the flow lines themselves, as they approach the streambed.

[4] Other studies have related stream water N concentrations to groundwater inputs. *Sprague et al.* [2000] found that 15–65% of the annual stream export of N from Chesapeake Bay watersheds was due to groundwater-based NO_3^- discharge into streams (i.e., NO_3^- transported into streams by groundwater seepage). In a study of 27 small watersheds in the Atlantic Coastal Plain, *Jordan et al.* [1997] found a positive correlation between annual flow-weighted mean NO_3^- concentration in stream water and the annual fraction of streamflow due to base flow; a negative correlation was found between dissolved organic N (DON) and base flow. Given the predominance of groundwater in base flow, these results suggest the potential significance of groundwater-based NO_3^- discharge to streams. They also suggest the opposite for DON (that the significant source to streams is overland flow, and groundwater inputs dilute this form of N), underscoring the importance of distinguishing among N species in attempts to assess hydrologic transport of N between groundwater and surface water.

[5] A number of studies focusing on N inputs and outputs in stream reaches, including some in which the main focus was on denitrification, have estimated N fluxes from groundwater to surface water (mass of N per unit area of streambed, per unit time) using a mass balance approach for a stream reach [e.g., *McMahon and Böhlke*, 1996; *Burns*, 1998; *Chestnut and McDowell*, 2000; *Böhlke et al.*, 2004; *Duff et al.*, 2008]. Other approaches not based on reach mass balance or stream water concentrations have been used to quantify NO_3^- flux from groundwater to surface water. For example, *Staver and Brinsfield* [1996] used data on hydraulic head, hydraulic conductivity, and NO_3^- concentrations measured in piezometers to calculate groundwater-based NO_3^- input to the Wye River from an agricultural area along one shoreline.

[6] The various approaches have advantages and disadvantages, with some of the latter probably arising when the main point of the study was other than quantifying N flux into the stream from groundwater. For example, in some studies focusing on denitrification and/or hyporheic mixing, groundwater-based NO_3^- input to the stream reach could not be distinguished from in-channel nitrification, creating uncertainty in the groundwater-based NO_3^- input [*Böhlke et al.*, 2004; *McMahon and Böhlke*, 1996]. In some cases NO_3^- concentration in groundwater was measured at relatively few points [*Burns*, 1998], or spatial/temporal information from many piezometers was combined by averaging concentrations over space and time [*Chestnut and McDowell*, 2000]. There are relatively few data on temporal variability,

the four repeated reach experiments of *Burns* [1998] and three of *Chestnut and McDowell* [2000] being significant exceptions (for the latter only the groundwater flow, not the groundwater NO_3^- concentration, varied temporally in the calculations). *Staver and Brinsfield* [1996] report an extensive temporal record of groundwater-based NO_3^- discharge to the Wye River (29 months of daily and monthly values); the extent of its applicability over space is not clear because the groundwater flux is based on data from only two piezometers.

[7] The environmental significance of groundwater-based N input to streams, and the difficulty in measuring it, argue for studies aimed specifically at this flux using a range of approaches. In this paper we describe work aimed at quantifying the coupled rates of groundwater and N flux through the streambed of a 0.26 km stream reach in North Carolina. We worked directly on the streambed in the reach instead of using a reach mass balance approach based on streamflow data (to, as far as possible, isolate the groundwater-based N input to the stream from other processes, and measure it as near as feasible to the groundwater-stream interface). Our field program involved repeated, spatially intensive (1) measurement of hydraulic head gradient (J) between the stream and the underlying groundwater, (2) sampling and chemical analysis of this streambed groundwater for NO_3^- , NH_4^+ , TDN, DON (TDN – NO_3^- – NH_4^+), dissolved O_2 , and several other chemical parameters, and (3) measurement of streambed hydraulic conductivity (K). The data were used to compute point values of water flux and N flux (for different N species) through the streambed. Interpolating and mapping these point values showed the spatial distributions of the linked water and N fluxes on the streambed, and allowed for comparison with the spatial distributions of potential controls such as J , K , and N concentration in groundwater. Total groundwater and groundwater-based N inputs to the study reach were also generated by spatial integration of interpolated flux fields on the streambed. Repeat measurements (bimonthly for a year) showed the temporal variability in the rates and patterns of streambed water and N fluxes.

2. Study Area

[8] The study was conducted within West Bear Creek watershed (61 km²), in a section of West Bear Creek approximately 6 km southeast of Goldsboro, North Carolina, United States (Figure 1). Elevation ranges from 22 to 40 m above sea level, mean annual precipitation is 1270 mm, and average monthly temperature ranges from 6.3°C in January to 27.3°C in July (<http://www.nc-climate.ncsu.edu/cronos/normals.php?station=313510>). Agriculture is the dominant land use within the watershed (~50% by area), and consists mainly of cotton, soybean, and corn [*Sherrell*, 2004; D. Gray, local farmer, personal communication, March 2007], with some wheat, tobacco, and cucumbers on the south side of the watershed (C. Wiggins, local farmer, personal communication, February 2008).

[9] West Bear Creek is a tributary to Bear Creek, which drains a heavily agricultural watershed [*Reckhow et al.*, 2004] and discharges a significant amount of N into the Neuse River [*Usry*, 2005]. The Neuse River is a major water resource for the region and the subject of numerous studies investigating the effects of N contamination in the river and

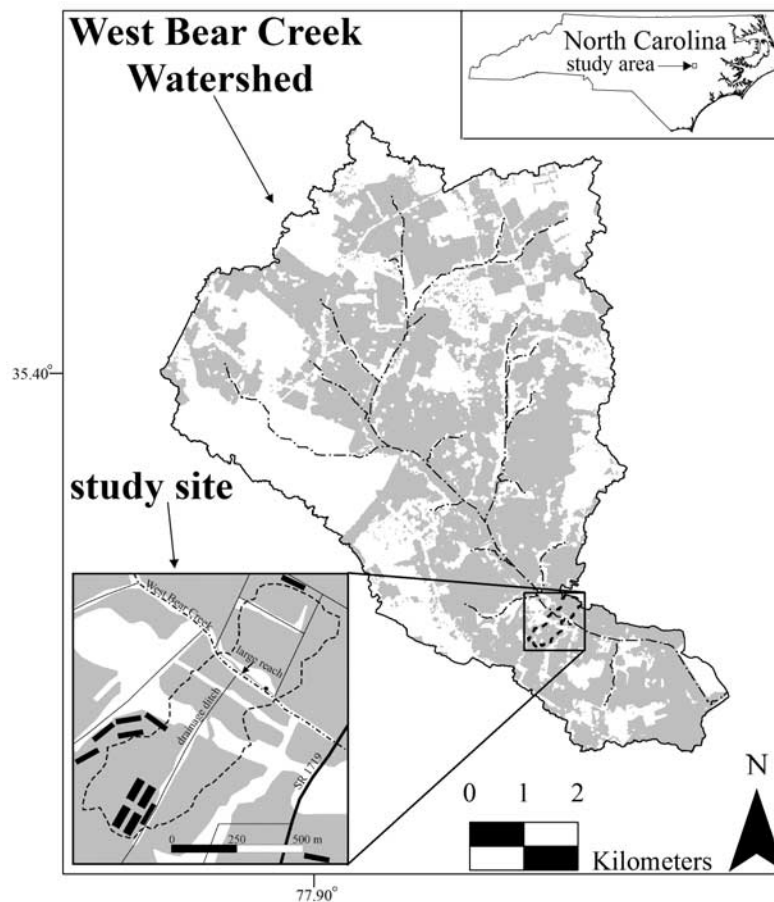


Figure 1. West Bear Creek watershed and location of study site. West Bear Creek is shown as a dash-dotted line, and the topographically defined contributing area of the 262.5-m “large” reach of West Bear Creek is outlined by the thick dashed line. Land use in the watershed is from U.S. Environmental Protection Agency (Land use data from Oct. 1998 to March 1999, available at <http://www.lib.ncsu.edu/gis/neusclu.html>), with gray portions of the watershed representing agriculture. Land use in the inset is based on a North Carolina Department of Transportation orthophotograph from 1998; agriculture is shown in gray, forested areas are shown in white, and farm buildings are shown by solid black rectangles. Land parcel boundaries are defined by thin black lines. Site of the Geoprobe[®] core is denoted by a black dot (350 m upstream of SR 1719).

its estuary [e.g., *Arhonditsis et al.*, 2007; *Stow et al.*, 2007; *Paerl et al.*, 2006; *Springer et al.*, 2005; *Fear et al.*, 2004; *Paerl et al.*, 1998]. Excessive N loading has led to degradation of surface water quality, eutrophication, and fish kills [e.g., *Burkholder et al.*, 1995; *Paerl*, 1997]. These effects have been attributed to nonpoint sources, of which agriculture is the largest (North Carolina Division of Water Quality, Total maximum daily load for total nitrogen to the Neuse River, North Carolina, 51 pp., 1999, available at http://www.esb.enr.state.nc.us/modeling_tmdlunit/PDFs/Neuse_TMDL_june.PDF). The North Carolina Environmental Management Commission adopted rules in 1997 to reduce N loading to the Neuse River by 30% (http://h2o.enr.state.nc.us/nps/Neuse_NSW_Rules.htm). Despite some N reduction over the past 10 years, the 30% reduction target has not yet been reached (North Carolina Division of Water Quality, 2007 Annual progress report of Neuse agriculture rule—Annual report to EMC-WQC, available at <http://h2o.enr.state.nc.us/nps/documents/NeuseAnnualReportFinal3b.pdf>).

[10] Our analysis of existing soils data (Soil Survey Staff, Natural Resources Conservation Service, U.S. Department of Agriculture, Soil survey of Wayne County, North Carolina, 2007, available at <http://websoilsurvey.nrcs.usda.gov/app/WebSoilSurvey.aspx>) indicates that soils in West Bear Creek watershed are mostly Ultisols (81%) and Inceptisols (13%); these soils overlie unconsolidated “surficial” siliclastics [*North Carolina Department of Transportation*, 2002; *North Carolina Department of Environment and Natural Resources*, http://www.ncwater.org/Data_and_Modeling/Ground_Water_Databases/frametable.php?countyname=WAYNE]. Beneath the surficial deposits lie the Cretaceous Black Creek and Tertiary Yorktown Formations [*North Carolina Geological Survey*, 1985] in the upper and lower halves of the watershed, respectively. Our study reach is in the portion of West Bear Creek underlain by the Black Creek formation.

[11] One small secondary drainage ditch discharges to the study reach (Figure 1); it flows intermittently for approximately 0.5 km through agricultural fields before reaching the stream. The study reach (and most of West Bear Creek)

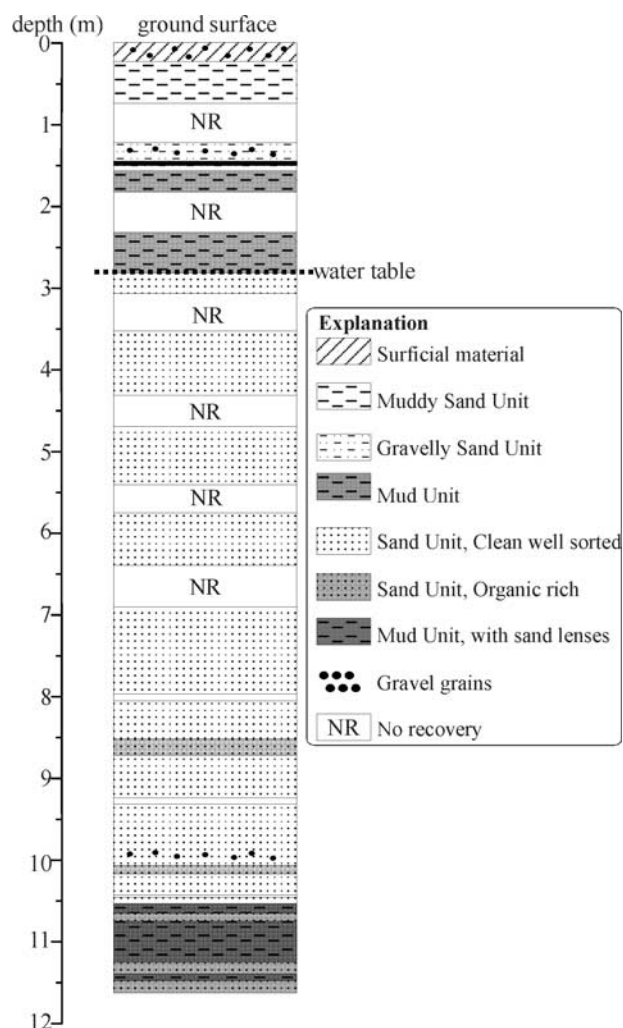


Figure 2. Stratigraphy of a Geoprobe® core collected on the north (left) side of West Bear Creek 350 m upstream of the State Road 1719 bridge [Elkins, 2007]. The thick unit of mostly sand and gravel is thought to represent the surficial aquifer, overlying what is likely the Black Creek aquitard.

was dredged and straightened in the 1950s (A. Miller, Division of Soil and Water Conservation, North Carolina Department of Environmental and Natural Resources, Wayne County, personal communication, August 2006) to facilitate drainage of the surrounding agricultural fields. The dredging has resulted in stream banks that are very steep and extend 2–3 m above the streambed on the left (north) side of the stream, the side on which the dredge spoils seem to have been placed. Both stream banks are covered with trees and shrubs, except for some very steep portions of the north bank which are grassy and/or bare. On the north bank, a grassy maintenance road parallels the stream and separates it from a wide row of dense vegetation that includes many large trees. Sieving of streambed sediment cores (0–36 cm) indicates that the streambed averages about 94% (by mass) sand, 0.05–2.0 mm [Genereux *et al.*, 2008], with small amounts of clay, silt, and gravel [Leahy, 2007], and organic matter (0 to 3% [Elkins, 2007]). Most of the sand (73% of the streambed on average) is in the medium to coarse size range, 0.25–1.0 mm [Leahy, 2007].

[12] A Geoprobe® core was collected on the north bank (left side) of West Bear Creek 350 m upstream of State Road (SR) 1719 on 23 January 2007 (Figures 1 and 2). Although full recovery of the core was not achieved, the general stratigraphy of the surficial aquifer and underlying confining layer were approximately identified. Surficial sediments consisted of sand and gravel with interbedded layers of mud and organic matter. The water table was located 2.8 m deep, near the bottom of a mud unit which overlies a 7.8-m thick sand unit. On the basis of the position of the water table and previous work on the hydrogeology of the North Carolina Coastal Plain [e.g., Winner and Coble, 1996], this sandy layer is thought to represent the surficial aquifer and the primary source of groundwater to West Bear Creek; the underlying mud unit (below 10.6 m) is interpreted as a lower confining layer (possibly the Black Creek aquitard).

[13] At the start of the study, stakes (PVC pipes 1.5 m in length and 3 cm in diameter) were driven into both stream banks to aid in defining and returning to measurement locations. The PVC stakes were spaced about 12.5 m apart on each stream bank, starting 300 m upstream of the upstream side of the SR 1719 bridge over West Bear Creek and running upstream over the full 262.5 m length of the study reach (Figures 1 and 3). The location of each PVC stake was determined with centimeter accuracy using a real-time kinematic (RTK) GPS survey, a technique that uses a dual frequency receiver and base station to determine geographic positions. The base station was placed on the SR 1719 bridge, and a nearby North Carolina Geological Survey benchmark was used to accurately determine the position of the base station.

3. Study Design

[14] Streambed measurements were made in three reaches of West Bear Creek (Figure 3 and Table 1). The “large reach” running from 300 to 562.5 m upstream of the SR 1719 bridge was the main focus of the study, including much of the work on spatial variability and all the work on temporal variability. Bimonthly measurements (Table 1) were made at 46 streambed points (Figure 3) from December 2005 through December 2006 (8 points were missed in December 2005).

[15] Also, closely spaced measurements were made once in each of two 62.5 m “small reaches” (Figure 3) that were part of the large reach (together they accounted for about 50% of the large reach). Data were collected in July 2006 in one reach (“July small reach”) and August 2006 in the other (“August small reach”), and the two were 300–362.5 m and 487.5–550 m upstream of the SR 1719 bridge, respectively. Data from the small reaches (Table 1) provided highly detailed one-time “snapshots” of spatial patterns in the streambed with a resolution about 5× greater than the measurements in the large reach. Genereux *et al.* [2008] discuss the spatial and temporal dynamics of K in these reaches, and Kennedy *et al.* [2009] discuss trace gas data, denitrification, and groundwater age for a 75-m section of the large reach.

[16] K and J measurements and groundwater sampling were done directly in the streambed. These “point measurements” (centimeter-to-decimeter-scale local measurements focused around a small slotted screen or field permeameter,

as discussed below) were used to calculate point values of groundwater and N flux through the streambed (groundwater flux was calculated as $v = JK$, and N flux as $f_N = v[N]$, where $[N]$ represents the concentration of a dissolved N species in streambed groundwater: TDN, NO_3^- , NH_4^+ , or DON). Point fluxes of water and N were then interpolated and mapped on

the streambed, and integrated over the area of the streambed (A) to calculate total rates of groundwater input ($Q_{GW} = \iint v dA$) and groundwater-based N input ($Q_N = \iint f_N dA$) to the reach (NO_3^- only for the small reaches, all N species for the large reach, Table 1). In all, physical and chemical data were collected at 422 points over the three reaches from December 2005 to December 2006. Each of the nine measurement runs (seven for the large reach and one for each of the two small reaches) required 2 days, with one exception: the December 2005 run in the large reach, which required 3 days.

[17] Streambed groundwater samples were collected in the interval 31–36 cm below the top of the streambed. This interval was used because it was attainable with the “piezomanometer” used for sampling (described in section 4), deep enough to provide a measurable hydraulic head difference between stream water and groundwater, and also deep enough to preclude the presence of stream water from “pumping” (stream water flow into the bed driven by an induced pressure distribution over bed forms) and “turnover exchange” (entrapment and release of pore water associated with scour and deposition as bed forms propagate) [Packman and Bencala, 2000] in this low-gradient stream [e.g., Grimm and Fisher, 1984; Thibodeaux and Boyle, 1987; Cerling *et al.*, 1990; Elliott and Brooks, 1997; Conant, 2004; Duff *et al.*, 2008]. Vertical profiles of chloride concentration in the streambed pore water measured at 23 locations in the large reach in April 2006 and June 2006 (using a 2-cm screen at depths of 18–20 cm, 33–35 cm, and 58–60 cm) showed little or no surface water mixing at a depth of 33–35 cm [Elkins, 2007]. Thus, water samples collected in this depth range in the streambed represent almost exclusively groundwater discharging to the stream rather than mixtures of this groundwater with stream water. If some groundwater NO_3^- is lost by denitrification in sediments above our sampling interval (31–36 cm) [e.g., Gu *et al.*, 2007, 2008], our reported values of $[\text{NO}_3^-]$ and f_{NO_3} represent upper limits. In cases where the most significant denitrification occurs in the top few mm of sediment (e.g., citations in section 4.4.1 of the review by Birgand *et al.* [2007]), conceptually and practically it may be best to view this loss more as in-channel nitrogen processing than as a reduction in the net groundwater-based nitrate flux into the stream.

[18] In the large reach, the measurement design consisted of three-point transects roughly normal to the axis of the stream channel (one measurement location in the center of the channel, one on the left side, and another on the right),

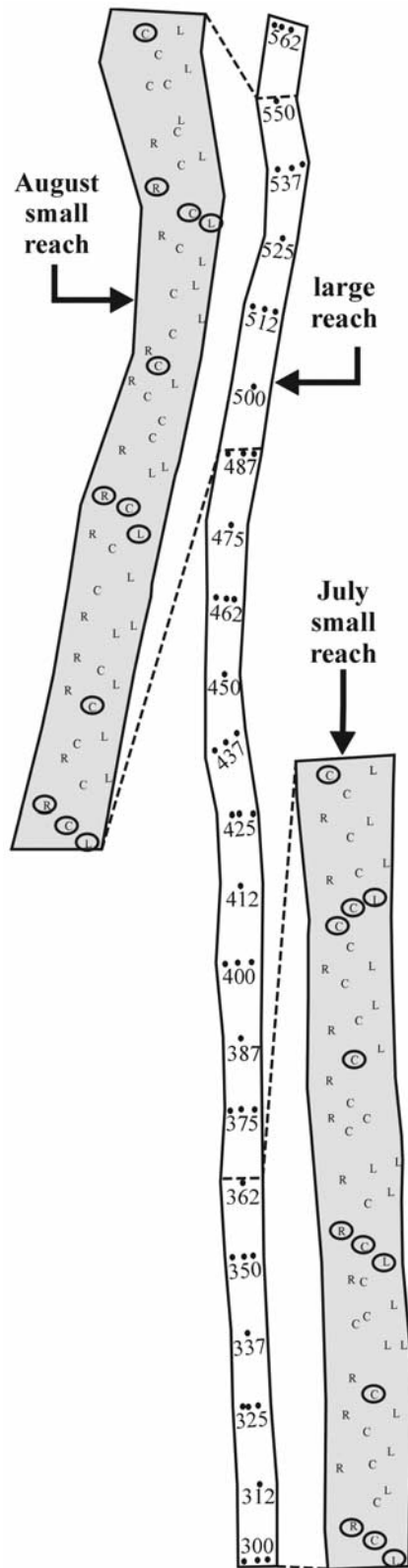


Figure 3. Sampling designs for the 262.5-m “large” reach and two 62.5-m “small” reaches (sampled in July and August 2006). For the large reach, black dots represent measurement points and numbers (e.g., 300, 312, and 325) refer to the distance in meters upstream of State Road 1719 (see Figure 1). For the small reaches, “L,” “C,” and “R” mark measurement points on the left side, center, and right side of the streambed, respectively. Circled points in the small reaches were used to estimate uncertainty in integrated inputs (see Appendix A). The direction of streamflow in the channel is from top to bottom in the figure; thus, the left side of the stream, defined as usual from the perspective of someone facing downstream, falls on the right side of the figure.

Table 1. Summary of Measurements in the Three Study Reaches

Parameter	Large Reach	Small Reaches ^a
Length (m)	262.5	62.5
Location ^b	300–562.5	300–362.5, ^c 487.5–550 ^d
Number of measurement points	46 ^e	54 (each reach)
Measurement density ^f	0.025	0.12, ^c 0.13 ^d
Time of measurement	bimonthly, Dec 2005 to Dec 2006	one Jul 2006, ^c the other Aug 2006 ^d
J	yes	yes
K	yes	yes
Temperature	yes	yes
pH	yes	yes
[O ₂]	yes	yes
[NO ₃ ⁻]	yes	yes
[NH ₄ ⁺]	yes	no
[DON]	yes	no

^aThere are two small reaches.^bLocation in West Bear Creek, in meters upstream of the upstream side of the State Road 1719 bridge (e.g., the large reach was 262.5 m long, from 300 to 562.5 m upstream of the bridge).^cJuly small reach.^dAugust small reach.^eThirty-eight in Dec 2005.^fMeasurement points per square meter of streambed.

spaced about 25 m apart along the channel, and a single measurement point in the center of the channel equidistant (12.5 m) from adjacent transects (Figure 3). Measurement points were named by their distance in meters from the upstream side of the SR 1719 bridge and a letter to indicate left side, center, or right side of the channel relative to the direction of streamflow (e.g., measurement point 375C is in the center of the channel, 375 m upstream of the SR 1719 bridge). When the study began there was a small beaver dam located about 3 m downstream of the measurement transect at 437 m in the large reach (Figure 3). The dam appeared in early November 2005 and persisted through the first 3 measurement runs (December 2005, February 2006, and April 2006), but had collapsed and was almost completely gone by June 2006.

[19] To initially mark and subsequently return on a bimonthly basis to the same measurement points in the large reach, we used the surveyed stream bank PVC stakes discussed in section 2. A tape measure was extended from the stake on the right bank (facing downstream) to the corresponding stake straight across the stream on the left bank. Measurement points were defined by their distances in cm from the right-bank stake. Returning to essentially the same measurement points is an important requirement for distinguishing temporal from spatial variability in a streambed that may be spatially heterogeneous over short distances, and so we paid close attention to relocating the same points within several cm.

[20] Dense measurement grids in the small reaches (Figure 3) were designed to achieve roughly even coverage over the streambed (as opposed to the closer lateral spacing and longer longitudinal or along-channel spacing in the large reach). To lay out these grids, a narrow stick about 60 cm in length and 2 mm in diameter was pushed into the sediment at each measurement point and its position (distance and azimuth) was determined relative to the nearest stream bank stake. Each stick was subsequently

removed as it was replaced in the streambed by a piezomanometer.

[21] Values of Q_{GW} and Q_N and contour maps of streambed attributes (e.g., J , v , f_{NO_3} , $[NO_3^-]$) were determined from raster grids (10-cm spacing) that were created in Surfer V.8[®] software with the multiquadratic radial basis function (MRBF) interpolation technique [Hardy, 1971; Carlson and Foley, 1991, 1992]. The “tension” or smoothness parameter (R^2 in SURFER) of the MRBF-interpolated surfaces was chosen such that the absolute mean error of the interpolation at the measurement points was equal to the mean uncertainty in the point values being interpolated (see Appendix A and Table S1 and Figure S1 in the auxiliary material).¹ Further details are in the work by Kennedy *et al.* [2008]. We introduced anisotropy in the interpolation and contouring process for the large reach. This creates a more realistic result when interpolation is carried out in a long narrow domain such as a surface water channel or a beach [Merwade *et al.*, 2006; Mitsova *et al.*, 2004], especially when the measurement spacing is much longer in the direction parallel to the long axis of the interpolation domain. Following Mitsova *et al.* [2004], we used an anisotropy ratio that was approximately equal to the ratio of longitudinal to lateral measurement spacing (in our case, 5); the longitudinal axis of the anisotropy was 50° counter-clockwise from north, the approximate average orientation of the nearly straight reach.

4. Field Measurements and Sample Collection

[22] A piezomanometer [Kennedy *et al.*, 2007] was used to measure J and collect streambed groundwater samples. J was calculated as the measured head difference between the streambed groundwater and the overlying stream water, divided by the distance from the top of the 5 cm piezomanometer screen to the top of the streambed (31 cm). At each measurement point, after determination of J , the piezomanometer was used to collect groundwater samples. Streambed groundwater was passed through a flow cell and temperature, specific conductance, [O₂], and pH were measured with a YSI model 556 multiprobe system. A sufficient volume of groundwater was purged to flush the sampling line and to achieve stability in these parameters (on average, 400–500 mL prior to collection of the first sample). Samples for analysis of cations (K⁺, Na⁺, Ca²⁺, Mg²⁺) and anions (Cl⁻, SO₄²⁻) were filtered to 0.7-μm (nominal) with precombusted Whatman GF/F filters and GF/D pre-filters in series and collected in 20-mL liquid scintillation vials; cation samples were acidified in the field with 10 μL of 2N HNO₃. For analysis of N species, samples were filtered as described above and collected in 30 mL HDPE bottles, acidified with 15 μL of 6N H₂SO₄ (for NO₃⁻ + NO₂⁻ and NH₄⁺ analysis) and unacidified (for TDN and NO₂⁻ analysis) (North Carolina Division of Water Quality, Collection and preservation of water quality samples, 2005, available at <http://h2o.enr.state.nc.us/lab/qa/collpreswq.htm>). Samples were kept in a cooler on ice in the field, and kept refrigerated (anions, cations, NO₃⁻ + NO₂⁻, and NH₄⁺) or frozen (TDN and NO₂⁻) in the laboratory prior to analysis.

¹Auxiliary materials are available in the HTML. doi:10.1029/2008WR007397.

[23] At each measurement point, streambed K was measured following measurement of J and collection of streambed groundwater. We used a standard falling-head field permeameter test [Genereux *et al.*, 2008] that has some sensitivity to horizontal K but is $\sim 30\times$ more sensitive to vertical K . K measurements refer to the top 36 cm of the streambed. For consecutive bimonthly measurement runs in the large reach, the piezomanometer was placed in the same location (within ~ 5 cm) at each measurement point, and the permeameter for K measurement was intentionally shifted by ~ 10 cm (upstream, downstream, or to the right or left) relative to the piezomanometer. This seemed a reasonable balance between returning to nearly the same points (to avoid confounding spatial and temporal variability) while also minimizing possible artifacts due to streambed disturbance by repeated K measurements at the exact same points.

[24] Volumetric streamflow was measured during each sampling day using a Pygmy current meter and the velocity-area technique [Herschy, 1995]. Stream width was fairly constant over the course of the study, with a mean and standard deviation (reflecting both spatial and temporal variability) of 7 ± 1 m ($n = 162$). Stream depth at the measurement points varied from 4 to 103 cm over the course of the study (mean and standard deviation were 35 ± 19 cm), and mean depths at the measurement points on the left side, center, and right side of the channel were within ± 1 cm of one another. Data were collected over a wide range of hydrologic conditions in the large reach, with measured streamflows ranging from $0.12 \text{ m}^3 \text{ s}^{-1}$ (August 2006) to $2.1 \text{ m}^3 \text{ s}^{-1}$ (December 2005). The degree of steadiness during each measurement run (generally 2 days) was assessed by comparing stream discharge (Q_{SW}) measured at the downstream end of the reach (site 300, Figure 3) at the start and end of the run. Differences in streamflow were $\leq 11\%$ for each of the first four runs (December 2005, February 2006, April 2006, and June 2006) and 21 and 24% for the October 2006 and December 2006 runs, respectively. For these six large-reach measurement runs, the temporal change in Q_{SW} over 2 days was about the same size as (or smaller than) the uncertainty in the change, and thus the magnitude of change is not precisely known but is relatively small. The August 2006 run is the one example of considerably less steady conditions due to a half-hour storm event around noon on the second sampling day; Q_{SW} was $0.12 \pm 0.02 \text{ m}^3 \text{ s}^{-1}$ at the start of the first day, and $0.28 \pm 0.03 \text{ m}^3 \text{ s}^{-1}$ at the end of the second day. For the small reaches, stream discharge was relatively steady during each 2-day field campaign, ranging from 0.82 ± 0.09 to $0.78 \pm 0.08 \text{ m}^3 \text{ s}^{-1}$ in July and from 0.11 ± 0.01 to $0.08 \pm 0.01 \text{ m}^3 \text{ s}^{-1}$ in August.

5. Chemical Analysis

[25] Samples were analyzed for TDN, $\text{NO}_3^- + \text{NO}_2^-$, NH_4^+ , and NO_2^- concentrations using standard methods [Eaton *et al.*, 2005; Merriam *et al.*, 1996], and for Cl^- and SO_4^{2-} concentrations by ion chromatography [U.S. Environmental Protection Agency (USEPA), 1993], in the Analytical Services Laboratory at North Carolina State University (<http://www.soil.ncsu.edu/services/asl/>), with analytical uncertainties ranging from 5 to 10%. Separate analyses of $[\text{NO}_2^-]$ in streambed groundwater samples from the first 3 measurement runs in the large reach (December 2005, February

2006, April 2006, 130 samples total) all had results below the limit of detection ($<7 \mu\text{M}$). Therefore, separate analyses of $[\text{NO}_2^-]$ were discontinued after April 2006, and all analyses of $[\text{NO}_3^- + \text{NO}_2^-]$ are reported as $[\text{NO}_3^-]$. Concentrations of cations were determined by inductively coupled plasma optical emission spectroscopy [USEPA, 1994] in the Geochemistry and Environmental Radioactivity Measurement Laboratory at East Carolina University with an analytical error of less than 5%.

6. Results and Discussion

6.1. K , J , and Groundwater Seepage Through the Streambed

[26] Mean streambed hydraulic conductivity K (all 422 measurements in the three reaches) was 18 m d^{-1} (Table 2), somewhat smaller than the mean streambed K values of $20\text{--}50 \text{ m d}^{-1}$ reported in other streams [Cey *et al.*, 1998; Cardenas and Zlotnik, 2003; Chen, 2004, 2005; Song *et al.*, 2007] but within the range expected for a streambed that is mostly medium to coarse sand. Streambed head gradient (J) ranged from -0.083 just upstream of the beaver dam (the negative value indicating downward flow into the streambed) to 0.27 (Table 2), similar to the range measured in agricultural streams in Ontario [Cey *et al.*, 1998] and Maryland [Böhlke and Denver, 1995]. Mean seepage rate ($v = KJ$) was 0.51 m d^{-1} (Table 2), similar to an agricultural stream in Ontario ($v = 0.43 \text{ m d}^{-1}$ [Cey *et al.*, 1998]) and larger than an agricultural stream in Indiana ($v = 0.17 \text{ m d}^{-1}$ [Böhlke *et al.*, 2004]).

[27] Emergent spatial and temporal relationships among K , J , and v are evident even with the considerable spatial variability in all three parameters. In general, areas of higher v coincide with areas of higher K , and the highest values of J were found only at points with very low K (Figures 4, 5, and S2). Similarly, Conant *et al.* [2004] found that the spatial variability of v in the streambed of Pine River (Ontario, Canada) was primarily a function of the wide range in streambed K . Other studies [e.g., Valett *et al.*, 1994; Chestnut and McDowell, 2000] have suggested that high J may serve as an indicator of high v in streambeds. In theory that may hold true if a streambed is homogeneous, but in West Bear Creek (and in Pine River, and, we believe, other typical heterogeneous streambeds) J cannot serve as a simple proxy for seepage rate v (Figure 6). Streambed maps of K , J , and v in the small reaches (Figure 5) show additional detail not evident in the large reach data (Figure 4) but do not give a fundamentally different picture of groundwater exchange with the stream.

[28] Lateral variability in K , J , and v across the channel was examined by comparing means of point values in the center of the channel to those on the left and right sides of the channel. Statistical t tests were performed to quantify the probability of the null hypothesis of no lateral variability (i.e., H_0 , $\bar{x}_{\text{left}} = \bar{x}_{\text{center}}$ and $\bar{x}_{\text{right}} = \bar{x}_{\text{center}}$ versus H_A , $\bar{x}_{\text{left}} \neq \bar{x}_{\text{center}}$ and $\bar{x}_{\text{right}} \neq \bar{x}_{\text{center}}$, where \bar{x} is mean K , J , or v , and left, center, and right correspond to position on the streambed). A significant difference was assigned to a t test resulting in a p value ≤ 0.05 [Zar, 1999, page 83].

[29] With the exception of the August small reach, average lateral variability in K and v generally followed a “center-high” pattern (higher values in the center of the

Table 2. Summary of Streambed Data^a

Statistic	Large Reach							Small Reach		All Reaches
	Dec 2005	Feb 2006	Apr 2006	Jun 2006	Aug 2006	Oct 2006	Dec 2006	Jul	Aug	
<i>T</i> (°C)										
Mean	12	14	16	19	21	16	14	21	20	17
SD	2	2	1	2	1	1	1	1	1	3
CV	15	11	7	9	5	6	6	5	4	19
Min.	8	10	14	10	19	13	13	19	19	8
Max.	15	17	18	21	24	18	17	24	21	24
<i>K</i> (m d ⁻¹)										
Mean	14.9	15.9	15.2	16.6	20.3	21.3	3.9	18.2	30.1	17.7
SD	12.6	13.9	13.0	15.4	16.1	16.5	4.8	14.1	17.9	15.7
CV	84	88	86	93	80	77	124	77	60	89
Min.	0.33	0.035	5.7 × 10 ⁻³	0.042	0.22	0.010	0.013	8.5 × 10 ⁻³	0.074	5.7 × 10 ⁻³
Max.	42.1	51.6	46.2	49.7	66.2	62.2	21.1	44.9	63.5	66.2
<i>J</i>										
Mean	0.042	0.036	0.043	0.036	0.043	0.058	0.064	0.037	0.056	0.046
SD	0.046	0.042	0.048	0.045	0.045	0.057	0.067	0.039	0.058	0.051
CV	110	116	114	124	105	98	105	103	103	110
Min.	-0.048	-0.083	-0.043	7.4 × 10 ⁻³	9.4 × 10 ⁻³	0.017	0.017	9.0 × 10 ⁻³	0.010	-0.083
Max.	0.23	0.17	0.20	0.19	0.19	0.25	0.24	0.26	0.27	0.27
<i>v</i> (m d ⁻¹)										
Mean	0.44	0.47	0.46	0.28	0.46	0.80	0.13	0.48	0.94	0.51
SD	0.50	0.58	0.48	0.26	0.32	0.59	0.15	0.39	0.72	0.53
CV	114	123	103	93	69	74	115	81	77	105
Min.	-0.51	-0.80	-0.16	7.1 × 10 ⁻³	0.021	2.8 × 10 ⁻⁴	5.7 × 10 ⁻⁴	1.7 × 10 ⁻⁴	0.020	-0.80
Max.	2.3	2.4	2.6	1.1	1.6	3.1	0.62	1.6	3.7	3.7
[TDN] (μM)										
Mean	391	390	382	406	530	516	445	ND	ND	438
SD	486	477	436	429	551	503	577	ND	ND	496
CV	124	122	114	105	104	98	129	ND	ND	113
Min.	<7	<7	<7	<7	<7	<7	<7	<7	<7	<7
Max.	1642	1578	1364	1499	1713	1499	1928	ND	ND	1928
[NO ₃ ⁻] (μM)										
Mean	330	334	372	402	449	473	370	475	665	437
SD	408	407	433	427	481	470	500	413	571	469
CV	124	122	116	106	107	99	135	87	86	107
Min.	<7	<7	<7	<7	<7	<7	<7	<7	<7	<7
Max.	1356	1342	1349	1499	1428	1356	1642	1499	1785	1785
%[TDN]	73	85	87	91	79	88	71	ND	ND	82
[DON] (μM)										
Mean	60	54	8	4	79	42	73	ND	ND	45
SD	81	94	10	12	93	46	118	ND	ND	80
CV	135	175	120	324	118	110	161	ND	ND	177
Min.	0	0	0	0	0	0	0	ND	ND	0
Max.	286	514	36	71	389	143	500	ND	ND	514
%[TDN]	24	10	10	5	21	11	25	ND	ND	15
<i>f</i> _{NO3} (mmol m ⁻² d ⁻¹)										
Mean	111	140	173	98	198	332	59	197	576	218
SD	209	262	378	161	341	450	147	258	760	413
CV	189	188	218	163	173	135	251	131	132	190
Min.	-145	-46	-38	0.025	0.22	0.11	4.1 × 10 ⁻³	1.6 × 10 ⁻³	1.0	-145
Max.	1086	1513	2465	767	2002	1549	791	930	3258	3258
% <i>f</i> _{TDN}	73	85	87	91	79	88	71	ND	ND	82
<i>f</i> _{DON} (mmol m ⁻² d ⁻¹)										
Mean	19	21	5.0	1.1	39	30	8.9	ND	ND	18
SD	42	47	14	4.0	80	51	20	ND	ND	46
CV	218	223	279	377	203	167	222	ND	ND	255
Min.	-23	-15	-1.5	0	0	0	0	ND	ND	-23
Max.	229	252	92	24	445	291	91	ND	ND	445
% <i>f</i> _{TDN}	24	10	10	5	21	11	25	ND	ND	15

^a*T*, groundwater temperature; SD, standard deviation; Max., maximum; Min., minimum; CV, coefficient of variation (%); %[TDN] and %*f*_{TDN} are equal to $\frac{1}{n} \sum_{i=1}^n ([x]/[TDN])_i$ and $\frac{1}{n} \sum_{i=1}^n (f_x/f_{TDN})_i$, respectively, where *x* is NO₃⁻ or DON and *n* is the number of samples. ND means no data.

channel, lower values toward the banks), whereas average lateral variability in *J* followed the opposite “center-low” pattern (Table 3 and Figure 6). The “center-high” pattern of *v* has been measured with seepage meters in streams in central Nebraska [Craig, 2005] and South Carolina

[Murdoch and Kelly, 2003]. In West Bear Creek, higher *K* in the center of the channel apparently focuses groundwater discharge toward the center, with important implications for the magnitude and spatial pattern of N flux through the streambed, because [NO₃⁻] is generally lower in the center

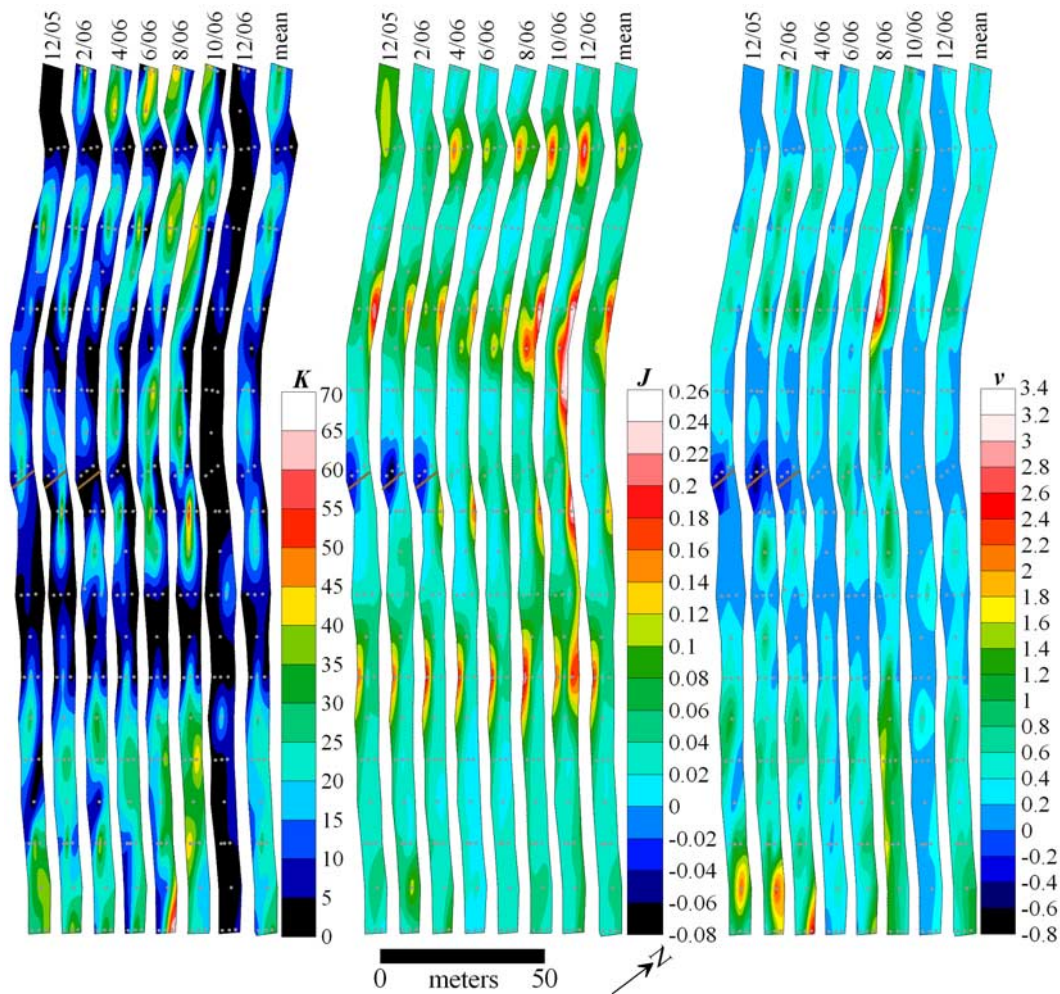


Figure 4. Contour maps of streambed K (m d^{-1}), J (dimensionless), and v (m d^{-1}) in the large reach: one map for each of the seven measurement runs and an eighth map for mean values over the entire study, December 2005 through December 2006. Small gray dots on the maps indicate the locations of the point values (38 locations for December 2005, 46 for all other maps). A brown line across the streambed marks the location of the beaver dam near the middle of the reach (present for December 2005, February 2006, and April 2006). The direction of streamflow in the channel is from top to bottom in the figure; thus, the left side of the stream, defined as usual from the perspective of someone facing downstream, falls on the right side of the figure.

of the channel (section 6.2). The generally higher K in the center of the channel is at least in part related to sediment dynamics in the channel [Genereux *et al.*, 2008], which in turn emerges as an important control on the coupled fluxes of water and N (sections 6.2 and 6.3) through the streambed.

[30] Variability in K , J , and v is due in part to a beaver dam that was present in the middle of the reach (immediately downstream of the transect labeled “437” in Figure 3) from December 2005 to April 2006. When the dam was present, mean values of K [Genereux *et al.*, 2008] and v upstream of the beaver dam were about 23 and 52%, respectively, lower than mean values downstream of the dam (differences significant at 80% confidence), and J was negative at the transect immediately upstream of the dam (Figure 4) indicating downward seepage into the streambed.

[31] General spatial patterns of K , J , and v were quite persistent through the study year (Figure 4). Zones of high and low values in the streambed remained in roughly the same areas but expanded and contracted with time, perhaps

in response to (1) changing hydrologic conditions that affected J and v , and (2) cycles of streambed deposition and erosion, or time-varying biological processes (bioturbation, biofilms, microbial gas production, and gas content of streambed sediments), that altered K [Genereux *et al.*, 2008]. As a quantitative index of temporal variability through the year in the large reach, correlation coefficients (r^2) were calculated for each attribute (K , J , v , and the NO_3^- concentrations and fluxes discussed in later sections) to compare each measurement run to the other 6 measurement runs. Results suggest that there is significant temporal variability in bimonthly results for K and v , but relatively less in J ; r^2 ranged from 0.03 to 0.51 for K (mean = 0.25), 0.01 to 0.56 for v (mean = 0.17), and 0.10 to 0.90 (mean = 0.56) for J . Some studies have estimated temporal variability in v by measuring J at different times but assuming a constant K [e.g., Cey *et al.*, 1998]. Although this may be a valid assumption in streams where erosion/deposition rates and other processes affecting K are small, it does not hold

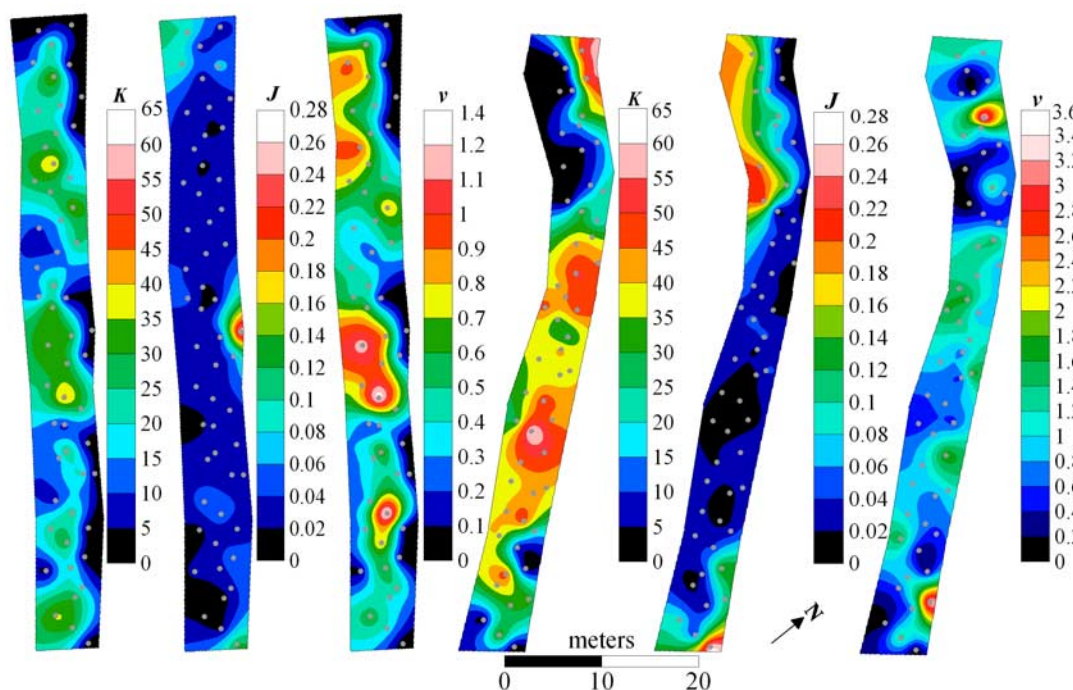


Figure 5. Contour maps of K (m d^{-1}), J (dimensionless), and v (m d^{-1}) for the July small reach (300–362.5 m upstream of SR 1719, three maps on the left) and August small reach (487.5–550 m upstream of SR 1719, three maps on the right). The direction of streamflow in the channel is from top to bottom in the figure; thus, the left side of the stream, defined as usual from the perspective of someone facing downstream, falls on the right side of the figure.

true for West Bear Creek (K varies on a bimonthly or shorter time scale).

[32] Q_{GW} to the large reach showed significant temporal variability, ranging from $251 \text{ m}^3 \text{ d}^{-1}$ to $1399 \text{ m}^3 \text{ d}^{-1}$ (Figure 7a). For each of the nine measurement runs (seven in the large reach, one in each small reach), Q_{GW} normalized by streambed area (Q_{GW}/A) was within 0–13% of the mean of the point values of v (mean difference was 4.7%; see Table S2), suggesting that, for the measurement program used, a mean streambed seepage rate for the reach can be determined by simple averaging of point values without the need for a complex spatial interpolation to determine Q_{GW} .

6.2. Nitrogen Concentrations in Streambed Groundwater

[33] On average 82% of TDN in streambed groundwater was in the form of NO_3^- (Table 2), with small but significant [DON] (averaging about 15% of [TDN]). Only a few samples (22 of 314) had $[\text{NH}_4^+]$ above the analytical detection limit (with concentrations of 8–56 μM), in agreement with the observation that $[\text{NH}_4^+]$ is typically low in agricultural recharge [Böhlke, 2002]. [DON] ranged from 0 to 514 μM and averaged 45 μM (Table 2).

[34] Over all 422 streambed measurement points, $[\text{NO}_3^-]$ in streambed groundwater ranged from <7 –1785 μM , with a mean of 437 μM (Table 2). In these same samples, $[\text{O}_2]$ ranged from 0.8 to 238 μM , or 0.3–91% air saturation at measured streambed groundwater temperature. Mean $[\text{O}_2]$ in streambed groundwater was 20 μM (7% of air saturation), with 42% of the samples having $[\text{O}_2] < 10 \mu\text{M}$. The combination of high $[\text{NO}_3^-]$ and low $[\text{O}_2]$ in groundwater is

fairly common in West Bear Creek but not in 4 other agricultural watersheds in the Atlantic Coastal Plain (Table 4). In the presence of an electron donor, denitrification usually occurs at about $[\text{O}_2] < 10 \mu\text{M}$ [Tiedje, 1988]. Thus, if these groundwater samples with low $[\text{O}_2]$ and high $[\text{NO}_3^-]$ have undergone some denitrification, it has obviously been incomplete (perhaps due to the absence of an electron donor, sufficient time, or some other factor). In a related paper [Kennedy *et al.*, 2009] we show that denitrification, although incomplete, is a significant factor in lowering the groundwater-based N input to West Bear Creek (on average, denitrification lowers f_{NO_3} by $\sim 50\%$ from what it would be in the absence of denitrification).

[35] Streambed $[\text{NO}_3^-]$ generally showed a “center-low” pattern (Figures 8, 9, and 10), with differences between the sides and center of channel statistically significant at 95% confidence for the large-reach (left versus center, and right versus center, average of all seven measurement runs) and the July and August small reaches (only for left versus center) (Table 3). Thus, low $[\text{NO}_3^-]$ usually coincided with high K and v in the center of the channel, with some exceptions (mean $[\text{NO}_3^-]$ on the right side and in the center were not significantly different at 95% confidence for the small reaches or for three of the seven individual large reach runs, on August 2006, October 2006, and December 2006). Contour maps of [DON] show the “center-low” pattern in some portions of the large reach (Figure 11), with one prominent exception near the upstream end of the reach on December 2006. Conant *et al.* [2004] also noted a relationship between concentration and lateral position on a streambed: they found high concentrations of volatile organic compounds (VOC) in streambed groundwater in the center

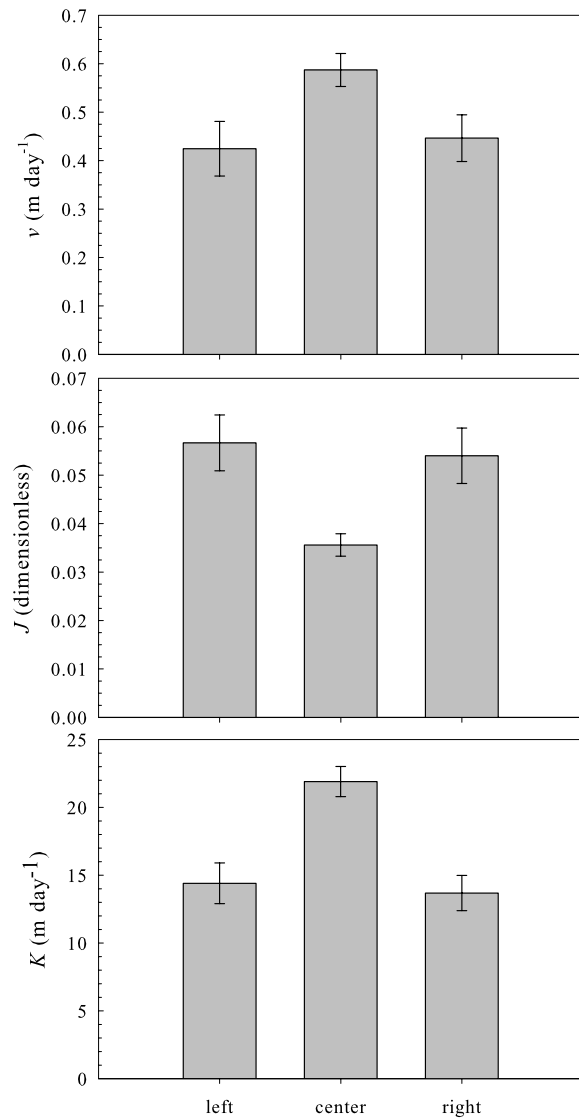


Figure 6. Arithmetic mean K , J , and v from the left side, center, and right side of the channel ($n = 422$). Errors bars are plus and minus one standard error of the mean.

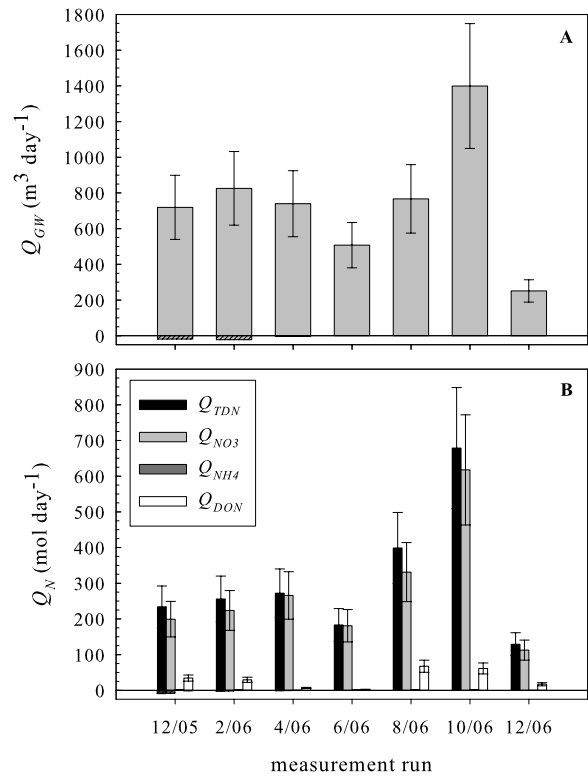


Figure 7. Integrated (a) groundwater seepage (Q_{GW}) and (b) groundwater-based N inputs (Q_N) to the large reach. Cross-hatched portions of the bars for the December 2005, February 2006, and April 2006 runs represent negative values immediately upstream of the beaver dam. Error bars represent an estimated 25% uncertainty (see Appendix A).

of the Pine River, and concluded it was due to the presence of relatively old groundwater beneath the center of the channel.

[36] The “center-low” pattern of $[\text{NO}_3^-]$ in streambed groundwater is consistent with both an increase in N use over time and the occurrence of older groundwater beneath the center of the channel [Kennedy *et al.*, 2009]. Conversations with local farmers and other agricultural professionals revealed that liquid N fertilizer has been applied to crops in West Bear Creek watershed since the 1970s and 1980s (K. Johnson, agricultural agent, North Carolina Coopera-

Table 3. Lateral Variability in the Means of Streambed Attributes^a

Attribute	Large Reach, $n = 314$					July Small Reach, $n = 54$					August Small Reach, $n = 54$					All Three Reaches, $n = 422$				
	L	C	R	L = C	R = C	L	C	R	L = C	R = C	L	C	R	L = C	R = C	L	C	R	L = C	R = C
T	16.0	16.1	16.1	0.69	0.81	21.1	20.9	21.6	0.33	0.03	19.9	19.6	20	0.24	0.11	17.4	17.1	17.2	0.43	0.80
K	11.0	20.3	11.0	<0.01	<0.01	10.4	25.0	17.0	<0.01	0.07	32.9	29.5	27.1	0.55	0.73	14.4	21.9	13.7	<0.01	<0.01
J	0.059	0.034	0.055	<0.01	<0.01	0.050	0.029	0.035	0.11	0.37	0.052	0.053	0.066	0.97	0.51	0.057	0.036	0.054	<0.01	<0.01
v	0.31	0.54	0.38	<0.01	0.02	0.26	0.63	0.52	<0.01	0.39	1.1	0.88	0.82	0.40	0.73	0.42	0.59	0.45	<0.01	0.02
$[\text{NO}_3^-]$	647	218	454	<0.01	<0.01	823	278	341	<0.01	0.59	874	491	656	0.05	0.35	710	256	465	<0.01	<0.01
f_{NO_3}	214	126	167	0.05	0.24	202	171	236	0.70	0.47	864	429	405	0.10	0.90	316	165	204	<0.01	0.30

^aColumns labeled L, C, and R give mean attribute values for the left side, center, and right side, respectively, of the streambed, in the following units: T is in $^{\circ}\text{C}$; K and v are in m d^{-1} ; J is dimensionless; $[\text{NO}_3^-]$ is in μM ; and f_{NO_3} is in $\text{mmol m}^{-2} \text{d}^{-1}$. Columns labeled L = C and R = C give p values from t tests for the significance of the difference between the left-side and center means and the right-side and center means, respectively (e.g., for f_{NO_3} in the large reach, probability that the left-side and center means are equal is 5%, and the probability that the right-side and center means are equal is 24%). Values for the large reach are means of all seven measurement runs from Dec 2005 to Dec 2006. As shown here, n is the number of measurement points.

Table 4. Comparison of O_2 and NO_3^- Concentrations in Streambed Groundwater in the Atlantic Coastal Plain, United States

Study	State	Number of Samples	$[\text{O}_2]$ (μM)		$[\text{NO}_3^-]$ (μM)	
			Mean	Range	Mean	Range
This study	NC	422	20	0.8–238	437	<7–1785
Böhlke and Denver [1995], CB ^a	MD	5	266	109–320	367	193–614
Modica et al. [1998]	NJ	33	129	19–250	346	4–1114
Böhlke and Denver [1995], MC ^b	MD	10	36	<2–300	58	<4–378
Tesoriero et al. [2005]	NC	9	22	3–34	8	<4–45

^aCB, Chesterville Branch watershed.^bMC, Morgan Creek watershed.

tive Extension, personal communication, June 2006; D. Gray, local farmer, personal communication, March 2007; J. Radford, Sleepy Creek Farms, personal communication, February 2008; J. T. Smith, local farmer, personal communication, February 2008; C. Wiggins, local farmer, personal communication, February 2008). Records of N fertilizer sales suggest increasing application of N fertilizer in the watershed since the 1950s [Kennedy et al., 2009].

[37] In the August small reach and the upstream half of the large reach, $[\text{NO}_3^-]$, $[\text{Ca}^{2+}]$, $[\text{K}^+]$, and $[\text{Cl}^-]$ were higher on the left (north) side of the streambed than on the right (Figures 8, 9, and S3), a pattern that may be related to the riparian buffer on the left side being thinner (a potential influence on NO_3^- if not the other solutes) and the farming practices being somewhat different on opposite sides of the channel [Kennedy et al., 2009]. Higher $[\text{NO}_3^-]$, $[\text{Ca}^{2+}]$, $[\text{K}^+]$, and $[\text{Cl}^-]$ in streambed groundwater on the left side of the streambed suggests that the most significant sources of agricultural chemicals to the stream are located on the north side of the channel. In this way, streambed groundwater may aid in identifying the relative locations of sources of groundwater-based contaminant inputs to a stream.

[38] Comparing each measurement run in the large reach to the other six measurement runs, values of $[\text{NO}_3^-]$ in streambed groundwater were well correlated over time; correlation coefficients (r^2) were 0.25–0.86 (mean = 0.60) for all seven runs. Results indicate that the physical attributes K and v are less self-correlated over time than $[\text{NO}_3^-]$; that is, there is less temporal variability in $[\text{NO}_3^-]$ than in K and v .

6.3. Groundwater-Based Nitrogen Inputs to West Bear Creek

[39] Nitrate and DON accounted for about 90 and 10%, respectively, of Q_{TDN} through the streambed into the reach (Table 5). Values of Q_{N} normalized by streambed area (Q_{N}/A) are similar to means of point values of f_{N} but are perhaps a more rigorous estimate of the true average streambed N flux for the reach. For each of the nine measurement runs (seven in the large reach, one in each small reach), Q_{NO_3}/A was within 1–13% of the mean of the point values of f_{NO_3} (mean difference was 5.9%; see Table S2), suggesting that, as with water flux, sampling design was generally sufficient to allow calculation of mean streambed nitrate flux into the reach by simple averaging of point values without the need for a complex spatial interpolation to determine Q_{NO_3} . Mean f_{NO_3} for all nine runs was $218 \text{ mmol m}^{-2} \text{ d}^{-1}$ (Table 2), somewhat higher than the mean f_{NO_3} of the large reach alone ($160 \text{ mmol m}^{-2} \text{ d}^{-1}$) because the small reaches were located in areas of relatively high f_{NO_3} within the large reach (Figures 8 and 9). Q_{DON}/A averaged $17 \text{ mmol m}^{-2} \text{ d}^{-1}$ for

the seven large reach measurement runs. The overall spatial variability in f_{NO_3} and f_{DON} , expressed as their coefficients of variation for individual measurement runs, was 131–251% and 167–377%, respectively (Table 2).

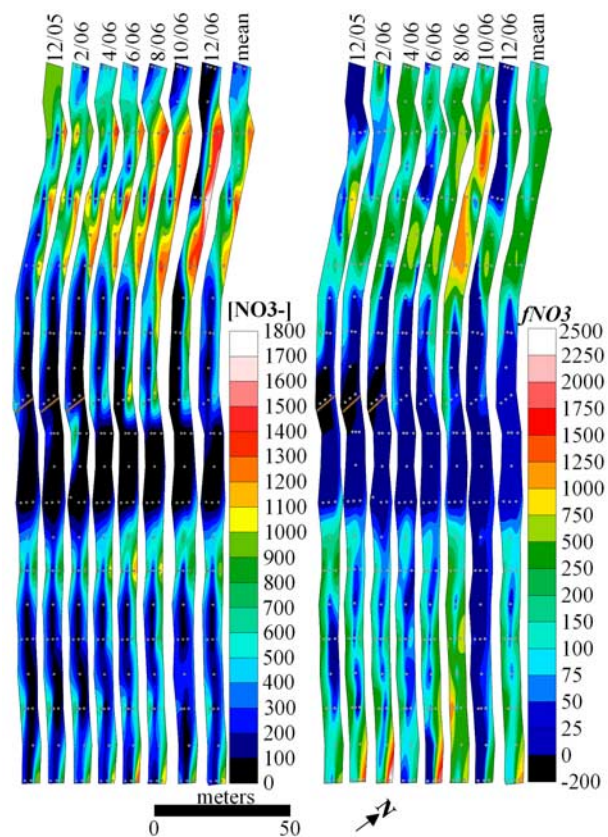


Figure 8. Maps of streambed $[\text{NO}_3^-]$ (μM) and f_{NO_3} ($\text{mmol m}^{-2} \text{ d}^{-1}$) in the large reach: one map for each of the seven measurement runs and an eighth map for mean values over the entire study, December 2005 through December 2006. Small gray dots on the maps indicate the locations of the point values (38 locations for December 2005, 46 for all other maps). A brown line across the streambed marks the location of the beaver dam near the middle of the reach (present for December 2005, February 2006, and April 2006). The direction of streamflow in the channel is from top to bottom in the figure; thus, the left side of the stream, defined as usual from the perspective of someone facing downstream, falls on the right side of the figure. Note the changes in contour interval for f_{NO_3} at 0, 100, and 250 $\text{mmol m}^{-2} \text{ d}^{-1}$.

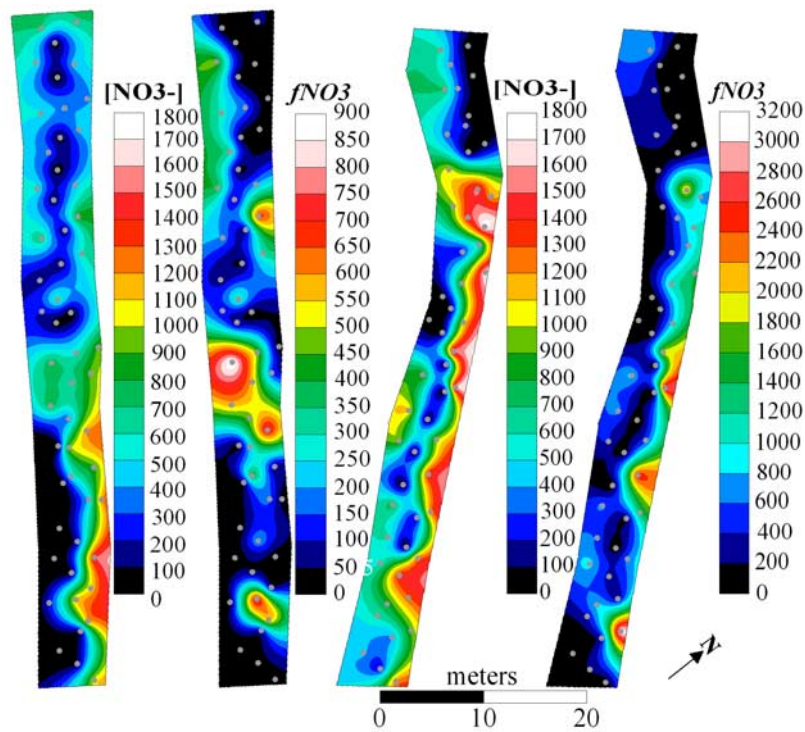


Figure 9. Contour maps of $[\text{NO}_3^-]$ (μM), and f_{NO_3} ($\text{mmol m}^{-2} \text{d}^{-1}$) for the July small reach (left two plots) and August small reach (right two plots). Small gray dots on the maps indicate the locations of the point values. The direction of streamflow in the channel is from top to bottom in the figure; thus, the left side of the stream, defined as usual from the perspective of someone facing downstream, falls on the right side of the figure.

[40] The large reach contained a broad zone of relatively low f_{NO_3} ($\leq 50 \text{ mmol m}^{-2} \text{d}^{-1}$) in the middle part of the reach and zones of higher f_{NO_3} at both the upstream and downstream ends of the reach (in the vicinity of the small reaches) (Figures 8 and 9). The zone of relatively low f_{NO_3} roughly surrounds the site of the beaver dam that existed during the first several months of the study (Figure 8). Negative seepage (downward into the streambed) just upstream of the dam (Figure 4) ceased after collapse of the dam, but the low $[\text{NO}_3^-]$ and f_{NO_3} near the dam (especially within about 40 m downstream) persisted (Figure 8), suggesting they may be due to factors other than the dam (or that any dam effects persisted for months after the collapse of the dam).

[41] Mean f_{NO_3} was generally lower in the center of the channel compared to the sides, with somewhat higher values on the left side than on the right (Figures 8–10), though the only center versus side differences that were significant at 95% confidence were those between the center and left side of the large reach (Table 3). Spatial variability in maps of f_{DON} is similar to that in maps of f_{NO_3} (Figures 8 and 11). On average, 70% of streambed nitrate flux into the large reach occurred in about 38% of the streambed area, 24% in 29% of the streambed, and the remaining 6% in 33% of the streambed. As mentioned earlier, streambed patterns of v are closely related to those of K , and those of K are controlled by physical (erosion, deposition) and possibly biological streambed processes [Genereux *et al.*, 2008]. The $[\text{NO}_3^-]$ of streambed groundwater is controlled largely by the history of fertilizer use in the watershed and denitrification [Kennedy *et al.*, 2009].

Thus, the spatial and temporal dynamics of f_{NO_3} are a complex function of both natural (physical, chemical, biological) and anthropogenic factors, and information on all of these factors was obtained by sampling in the streambed, as discussed here and in the two papers cited above.

[42] The mean value of f_{NO_3} in the August small reach was significantly higher than those in the July small reach and any of the 7 large reach measurement runs (Table 2), further illustrating how the August small reach differed from the other reaches (in addition to the previously mentioned lack of “center-low” and “center-high” lateral variability in K , J , and v in the August small reach). Thus, significant portions of the streambed (62.5 m, in this case) may exhibit streambed water and N fluxes (v , f_{NO_3}) and other attributes with significantly different means and spatial distributions from much larger sections of streambed (e.g., the 0.26 km large reach).

[43] Values of Q_{NO_3} were 112–618 mol d^{-1} (mean of 274 mol d^{-1}) for the large reach (Figure 7b). Q_{NO_3} was 83–99% of Q_{TDN} to the large reach, and DON was 1–17% (2–67 mol d^{-1}). For the large reach, very low $[\text{NH}_4^+]$ resulted in values of Q_{NH_4} that were $\leq 0.2\%$ of Q_{TDN} , ranging from -0.4 to 0.9 mol d^{-1} . For the first three measurement runs (December 2005, February 2006, and April 2006), small negative values of Q_{NO_3} ranging from -0.7 to -8.1 mol d^{-1} were calculated immediately upstream of the beaver dam, where negative values of J were measured. Temporal variability in Q_{NO_3} of the large reach appears to be controlled more by changes in Q_{GW} (Figures 7a and 7b) than by changes in $[\text{NO}_3^-]$ (Table 2). The similarity of the temporal

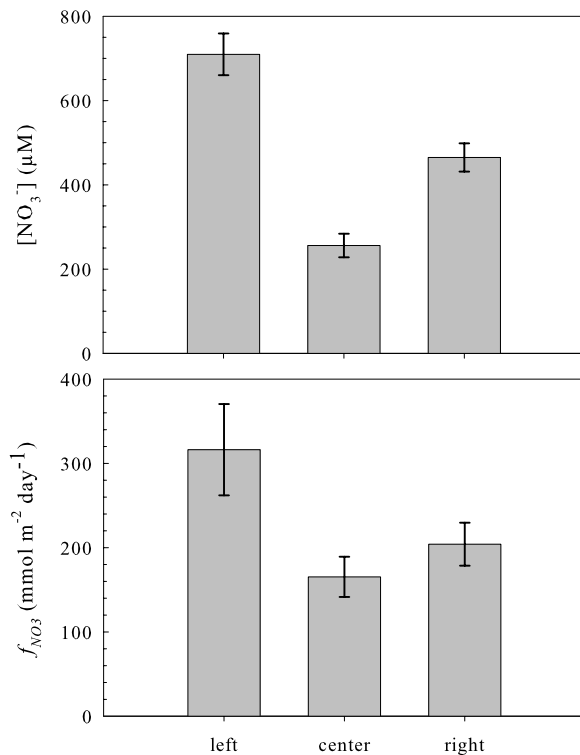


Figure 10. Arithmetic mean $[\text{NO}_3^-]$ of streambed groundwater and f_{NO_3} from the left side, center, and right side of the channel ($n = 422$). Error bars are plus and minus one standard error of the mean.

variability in Q_{GW} and Q_{NO_3} , and greater temporal similarity between f_{NO_3} and v than between f_{NO_3} and $[\text{NO}_3^-]$ (Table 2), suggest that over the course of the study the temporal variability in groundwater-based nitrate flux into the stream was more closely controlled by changes in groundwater seepage than by changes in $[\text{NO}_3^-]$ in streambed groundwater.

[44] It is possible that sediment erosion and deposition is behind the large change in K , v , and f_{NO_3} in the large reach from October to December 2006 (Figures 4, 7, and 8 and Table 2). As discussed by *Genereux et al.* [2008], there were relatively large changes in the elevation of the streambed surface during this period (e.g., erosion at 300 m, deposition at 437 m; locations shown in Figure 3). Also, at the nearest continuous stream discharge measurement site (about 5 km downstream of the study reach), a large multipeak hydrograph (with the 2nd and 3rd largest peak flows of 2006) was recorded in late November, several days before the December 2006 K measurements [*Leahy, 2007*]. Changes in mean head gradient J (10% increase) and the $[\text{NO}_3^-]$ of streambed groundwater (22% decrease) from October 2006 to December 2006 were relatively small compared to the decreases in K , v , and f_{NO_3} (factors of 5.5, 6.2, and 5.6, respectively; see Table 2). In other words, neither J nor $[\text{NO}_3^-]$ data capture or reflect the largest temporal change in streambed water and N flux during the study year, and that change is consistent with the drop in streambed K .

[45] Mean NO_3^- flux through the streambed of West Bear Creek, whether calculated as Q_{NO_3}/A or as the mean of f_{NO_3}

point values, is within the range of f_{NO_3} found for other agricultural sites (Table 5). Differences among studies could be in part due to differences in methods, such as how groundwater seepage and $[\text{NO}_3^-]$ were determined, as well as to land use or other site differences. Many studies [e.g., *Burns, 1998*; *Chestnut and McDowell, 2000*; *McCutchan et al., 2003*] have used riparian groundwater from wells to define the $[\text{NO}_3^-]$ of groundwater seepage to a stream, but this approach may overestimate groundwater-based NO_3^- input to the stream if denitrification or other biogeochemical processes take place along the groundwater flow path between the riparian well and the top of the streambed. For example, in a related study [*Kennedy et al., 2009*], mean $[\text{NO}_3^-]$ from two riparian wells sampled from the lower part of the large reach in April 2007 was 35% higher (489 μM) than the mean of the 21 streambed groundwater

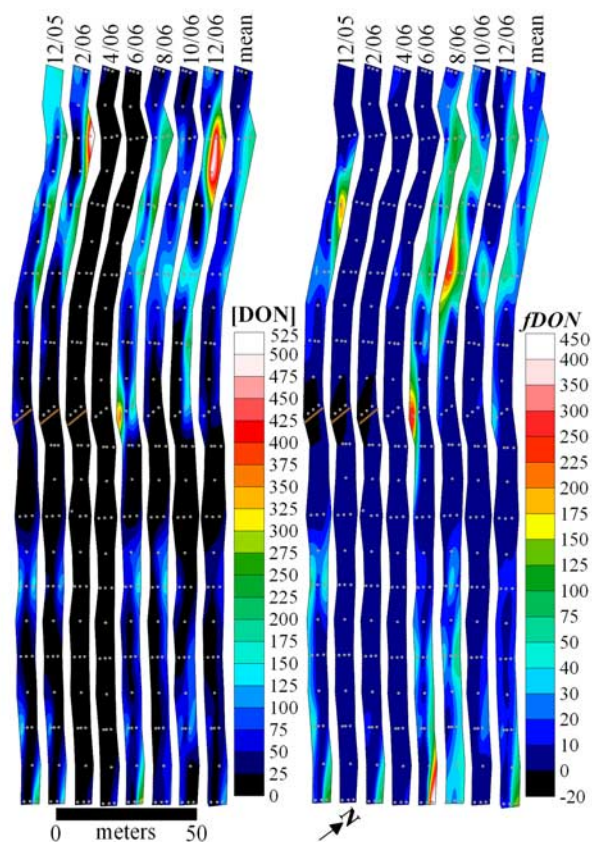


Figure 11. Maps of streambed $[\text{DON}]$ (μM) and f_{DON} (mmol m⁻² d⁻¹) in the large reach: one map for each of the seven measurement runs and an eighth map for mean values over the entire study, December 2005 through December 2006. Small gray dots on the maps indicate the locations of the point values (38 locations for December 2005, 46 for all other maps). A brown line across the streambed marks the location of the beaver dam near the middle of the reach (present for December 2005, February 2006, and April 2006). The direction of streamflow in the channel is from top to bottom in the figure; thus, the left side of the stream, defined as usual from the perspective of someone facing downstream, falls on the right side of the figure. Note the three changes in contour interval in f_{DON} at 0, 50, and 250 mmol m⁻² d⁻¹.

Table 5. Comparison of Estimates of Groundwater-Based N Fluxes Through Streambeds, f_N

	Type ^a	f_N (mmol d ⁻¹ m ⁻²) ^b			
		TDN	NO ₃ ⁻	NH ₄ ⁺	DON
This study ^c	Ag	171	154	1.5	17
Böhlke <i>et al.</i> [2004] ^d	Ag	ND	≤19	ND	ND
Burns [1998] ^e	F	ND	25	ND	ND
Chestnut and McDowell [2000] ^f	F	70	1.3	62	7.7
Duff <i>et al.</i> [2008], ^g DR2	Ag	ND	267	ND	ND
Duff <i>et al.</i> [2008], ^g Maple Cr	Ag	ND	11	ND	ND
Duff <i>et al.</i> [2008], ^g Morgan Cr	Ag	ND	262	ND	ND
McMahon and Böhlke [1996] ^h	Ag	ND	205	ND	ND
McCutchan <i>et al.</i> [2003] ⁱ	Ag	ND	87	10	ND
Staver and Brinsfield [1996] ^j	Ag	ND	158	ND	ND

^aAg, agricultural watershed; F, forested watershed.^bND means no data.^cWe estimated f_N as the mean of Q_N/A (Figure 7b) for the seven large reach measurements runs.^dWe estimated f_{NO_3} as $Q_{GW} = 881 \text{ m}^3 \text{ d}^{-1}$ (from a reach water budget) times $[NO_3^-] = 115 \text{ } \mu\text{M}$ divided by $A = 5400 \text{ m}^2$ [Böhlke *et al.*, 2004, Table 1]; f_{NO_3} is given as an upper limit because it could not be reliably distinguished from nitrification, another source of NO_3^- .^eIn this study, f_{NO_3} is an average of four values (ranging from 10 to 46 mmol m⁻² d⁻¹) we estimated in the upper reach (from data in Table 3 of Burns [1998]), using $A = 967 \text{ m}^2$, based on the reach length of 586 m and width of 1.65 m [Burns, 1998, Table 1], and the sampling period of 2 days.^fWe estimated f_{NO_3} as the mean $Q_{GW} = 135 \text{ m}^3 \text{ d}^{-1}$ (average of three values in Table 3 of Chestnut and McDowell [2000]) times mean $[NO_3^-]$ riparian groundwater at 1 m from the stream [Chestnut and McDowell, 2000, Table 2], using $A = 150 \text{ m}^2$, on the basis of the reach length of 100 m and width of 1.5 m.^gWe estimated f_{NO_3} as Q_{NO_3}/A [Duff *et al.*, 2008, Tables 1 and 5] for three sites in Washington (DR2), Nebraska (Maple Cr), and Maryland (Morgan Cr).^hWe estimated f_{NO_3} as Q_{NO_3} (123 kmol d⁻¹, from their NO_3^- mass balance for the river reach) divided by $A = 6 \times 10^5 \text{ m}^2$ (using Figure 2 of McMahon and Böhlke [1996] to estimate the river width as 80 m for the 7.5 km long reach).ⁱWe estimated f_N as $Q_{GW}/A = 0.2 \text{ m d}^{-1}$ (from a reach water budget and riverbed area) times $[NO_3^-]$ and $[NH_4^+]$ concentrations in groundwater collected from piezometers adjacent to the reach (436 and 52 μM , respectively) [McCutchan *et al.*, 2003, Table 2].^jWe estimated f_{NO_3} as an average of two annual values from consecutive years (153 and 163 mmol m⁻² d⁻¹), calculated using measurements of K , J , and $[NO_3^-]$.

measurements in the same portion of the reach at the same time (362 μM).

[46] Finally, we compared two estimates of flow-weighted mean $[NO_3^-]$ in streambed groundwater to each other and to the simple unweighted mean $[NO_3^-]$, to address three practical questions related to quantifying average $[NO_3^-]$ in groundwater seepage to a stream: (1) Does it matter if measured $[NO_3^-]$ is weighted by groundwater seepage rate? (2) If so, how much does it matter? (3) Are flow-weighted values of $[NO_3^-]$ dependent upon which method is used? The two estimates of flow-weighted mean (where the weighting was by the groundwater flow rate v through the streambed) were calculated as $[NO_3^-]_{\text{FWM}} = Q_{NO_3}/Q_{\text{GW}}$ and $[NO_3^-]_{\text{FWM}} = \sum f_{NO_3}/\sum v$. The former estimate relies on integration over interpolated fields of v and f_{NO_3} on the streambed (required to generate Q_{NO_3} and Q_{GW}) and more explicitly connects f_{NO_3} point values and associated streambed areas; the latter estimate does not require spatial interpolation and integration (only summation of point values) and is therefore easier to calculate. Differences between the two estimates of flow-weighted mean $[NO_3^-]$

were small (0.6 to 7%, mean of 3.5%, Table S2) and neither was consistently higher or lower, suggesting either approach to weighting may be used. For eight of the nine measurement runs (excluding December 2006), Q_{NO_3}/Q_{GW} was 3.2–17% lower (mean = 9.7%, Table S2) than unweighted mean $[NO_3^-]$ (changes in K just before December 2006 seem to have altered the relationship between v and $[NO_3^-]$ on the streambed, such that the unweighted mean $[NO_3^-]$ was actually about 17% higher, Table S2). While the answer to question 1 above is apparently “yes,” it could have been “no” if v and $[NO_3^-]$ had not been correlated in the streambed (it was “yes” largely because of the confluence of higher v and lower $[NO_3^-]$ in the center of the streambed, something discovered only because J , K , and $[NO_3^-]$ were all measured at the same numerous streambed points). This reinforces the value of simultaneous determination of both v and $[NO_3^-]$ in the streambed.

7. Summary and Conclusions

[47] The coupled groundwater and nitrogen (N) fluxes through the streambed of West Bear Creek were quantified, at the point scale and for reaches of about 62 to 262 m, using simultaneous measurements of streambed hydraulic conductivity (K) and hydraulic head gradient (J), and the concentrations of NO_3^- and other dissolved N species in the streambed groundwater. Data were collected at 422 streambed measurement points on nine 2–3 day measurement runs between December 2005 and December 2006, over a range of hydrologic conditions (stream discharge from 0.08 to 2.1 m³ s⁻¹), and the streambed variables (K , J , water flux $v = KJ$, N concentrations, and N fluxes calculated as the product of v and concentration) were interpolated, mapped, and (for the fluxes) integrated over the streambed. The resultant maps (Figures 4, 5, 8, 9, and 11) show the spatial distributions of these variables on the streambed and their relation to each other. Repeat measurements show the temporal variability in these distributions, and in the integrated water and N inputs to the large (262.5 m) reach.

[48] N fluxes through the streambed (f_N , mmol m⁻² d⁻¹) were generally lower in the center of the channel and higher on the sides, the same pattern shown (with some exceptions) by J and $[NO_3^-]$ but opposite to that of K and v (Figures 4–6 and 8–10). Higher K in the center of the channel is associated with lower silt and clay content in the streambed sediment [Genereux *et al.*, 2008], which is likely related to higher stream water velocity near the center of the channel and possibly other aspects of sediment dynamics. The $[NO_3^-]$ of streambed groundwater is controlled largely by groundwater age, the history of fertilizer use in the watershed, and denitrification [Kennedy *et al.*, 2009]. Thus, the spatial and temporal dynamics of NO_3^- flux through the streambed, $f_{NO_3} = v[NO_3^-]$, are a function of both natural (physical, chemical, and biological) and anthropogenic factors. Differences in N use on the north and south sides of the study stream may contribute to the asymmetrical lateral distributions of $[NO_3^-]$ and f_{NO_3} (Figure 10), though modeling of dissolved gas data from the site suggests that greater denitrification on the right side of the stream also plays a role [Kennedy *et al.*, 2009]; the physical hydrologic attributes (K , J , and v) have much more symmetrical lateral distributions in the streambed (Figure 6).

[49] With regard to linked spatial and temporal variability, f_{NO_3} was characterized by localized zones of high and low values that changed in size and shape over time but remained in basically the same locations, with 70% of NO_3^- flux to the large reach seeping through about 38% of the streambed, 24% through 29% of the streambed, and the remaining 6 through 33% of the streambed. The persistence of spatial patterns over time was similar for the other streambed attributes, especially K , J , and $[\text{NO}_3^-]$ (Figures 4 and 8); v seems to show the greatest deviation from this, and largest temporal variability overall (Figure 4). These results illustrate the importance of field sampling at fine spatial scales as a means to resolve localized “hot spots” of N flux in the streambed and assess the controlling influences on these fluxes by K , J , concentration, and, as in the work by Kennedy *et al.* [2009], denitrification and groundwater age.

[50] The dominant control on the temporal variability in f_{NO_3} was v (not $[\text{NO}_3^-]$), and transient changes in v were controlled by changes in both K and J . In studies of streambed fluxes, changes in J are routinely measured and understood as the result of changing hydrologic conditions on a watershed, but changes in streambed K have not received similar attention. Models of transient groundwater–surface water N exchange focusing on temporal changes in J have been developed [e.g., Gu *et al.*, 2008], but incorporating temporal variation in K may allow new insights and a more realistic simulation of streambed fluxes in some natural streams.

[51] The work presented here shows a practical means of using streambed data to quantitatively answer the question, “What is the rate of N transport from groundwater to surface water?” While the reach mass balance approach used in previous work is an important tool and should continue to see use, the approach taken here also has advantages, including: (1) showing directly the spatial and temporal dynamics of N fluxes on the streambed, and their relation to various controlling factors, (K , J , N concentration, groundwater age, etc.) (2) a fairly clear separation between groundwater-based N input and other processes affecting N in the stream (e.g., nitrification), and (3) the potential to estimate groundwater-based N input to a stream reach even in the presence of a very small relative increase in streamflow rate from the upstream end to the downstream end of the reach (a potentially serious problem for reach mass balance).

Appendix A

[52] Uncertainty in v and f_N was based on propagation, using standard methods [Kennedy *et al.*, 2007, and references therein], of the 95% uncertainties in K and J (for v), and v and $[\text{N}]$ (for f_N). Uncertainty in K (averaging about 20%) is discussed in detail by Genereux *et al.* [2008] (Table S1 and Figure S1). Uncertainty in J was estimated from uncertainty in the measurands Δh , L , and an amplification factor (AF) used to convert measured (“amplified”) oil:water manometer readings of Δh to the actual values of Δh in mm of water [Kennedy *et al.*, 2007], and averages about 5% (Table S1).

[53] Uncertainty in $[\text{N}]$ (dissolved aqueous concentrations of TDN, NO_3^- , NO_2^- , and NH_4^+) reported by the laboratory was 5% for concentrations greater than about 140 μM and

10% for lower concentrations. For values below the detection limit of 7 μM , half the detection limit (3.5 μM) was used for $[\text{NO}_3^-]$ and $[\text{TDN}]$, and 0 μM was used for $[\text{NH}_4^+]$. All uncertainties were expressed as 95% confidence intervals. On the basis of all 422 point values, mean relative uncertainty (uncertainty in each value divided by the value) was 17% for the groundwater seepage flux v and 24% for the two largest N fluxes, f_{TDN} and f_{NO_3} (Table S1).

[54] To estimate uncertainty in Q_{GW} and Q_N (the spatial integrals of v and f_N), we compared values of Q_{GW} and Q_N calculated in two different ways for each small reach: using all 54 point values, and using only 12 points that fell near large reach measurement points (the latter mimics the lower measurement density in the large reach). This approach assumes streambed measurement density is a key variable controlling the uncertainty in whole-reach quantities derived from streambed measurements, an assumption supported by previous analysis of the small reach data [Kennedy *et al.*, 2008]. Using this approach, differences in Q_{GW} and Q_N (based on high versus low measurement density) were –36% and –7%, respectively, for the July small reach, and 18% for the both Q_{GW} and Q_N in the August small reach. Thus, it is probably reasonable to conclude that average uncertainty in Q_{GW} and Q_N is about 20–25%.

[55] **Acknowledgments.** The authors gratefully acknowledge financial support of this work by the U.S. Department of Agriculture Cooperative State Research, Education, and Extension Service (USDA CSREES) award 2003-35102-13656. Brad Elkins, Lisa Cowart, and Kat Marciniak provided valuable assistance with the field data collection. Dave Bernstein of Geodynamics, LLC, generously conducted the real-time kinematic GPS survey of the stream bank stakes. We are especially grateful to the associate editor, two anonymous referees, and Peter McMahon, who provided numerous comments and suggestions, resulting in an improved manuscript.

References

- Arhonditsis, G. B., C. A. Stow, H. W. Paerl, L. M. Valdes-Weaver, L. J. Steinberg, and K. H. Reckhow (2007), Delineation of the role of nutrient dynamics and hydrologic forcing on phytoplankton patterns along a freshwater-marine continuum, *Ecol. Modell.*, **208**, 230–246, doi:10.1016/j.ecolmodel.2007.06.010.
- Birgand, F., R. W. Skaggs, G. M. Chescheir, and J. W. Gilliam (2007), Nitrogen removal in streams of agricultural catchments—A literature review, *Crit. Rev. Environ. Sci. Technol.*, **37**, 381–487, doi:10.1080/10643380600966426.
- Boesch, D. F., R. B. Brinsfield, and R. E. Magnien (2001), Chesapeake Bay eutrophication: Scientific understanding, ecosystem restoration, and challenges for agriculture, *J. Environ. Qual.*, **30**, 303–320.
- Böhlke, J. K. (2002), Groundwater recharge and agricultural contamination, *Hydrogeol. J.*, **10**(1), 153–179, doi:10.1007/s10040-001-0183-3.
- Böhlke, J. K., and J. M. Denver (1995), Combined use of groundwater dating, chemical, and isotopic analyses to resolve the history and fate of nitrate contamination in two agricultural watersheds, Atlantic Coastal Plain, Maryland, *Water Resour. Res.*, **31**(9), 2319–2339, doi:10.1029/95WR01584.
- Böhlke, J. K., R. Wanty, M. Tuttle, G. Delin, and M. Landon (2002), Denitrification in the recharge area and discharge area of a transient agricultural nitrate plume in a glacial outwash sand aquifer, Minnesota, *Water Resour. Res.*, **38**(7), 1105, doi:10.1029/2001WR000663.
- Böhlke, J. K., J. W. Harvey, and M. A. Voytek (2004), Reach-scale isotope tracer experiment to quantify denitrification and related processes in a nitrate-rich stream, midcontinent United States, *Limnol. Oceanogr.*, **49**(3), 821–838.
- Burkholder, J. M., H. B. Glasgow Jr., and C. W. Hobbs (1995), Fish kills linked to a toxic ambush-predator dinoflagellate: Distribution and environmental conditions, *Mar. Ecol. Prog. Ser.*, **124**, 43–61, doi:10.3354/meps124043.
- Burns, D. A. (1998), Retention of NO_3^- in an upland stream environment: A mass balance approach, *Biogeochemistry*, **40**, 73–96, doi:10.1023/A:1005916102026.

- Cardenas, M. B., and V. A. Zlotnik (2003), Three-dimensional model of modern channel bend deposits, *Water Resour. Res.*, 39(6), 1141, doi:10.1029/2002WR001383.
- Carlson, R. E., and T. A. Foley (1991), The parameter R^2 in multiquadratic interpolation, *Comput. Math. Appl.*, 21(9), 29–42, doi:10.1016/0898-1221(91)90123-L.
- Carlson, R. E., and T. A. Foley (1992), Interpolation of track data with radial basis methods, *Comput. Math. Appl.*, 24(12), 27–34, doi:10.1016/0898-1221(92)90169-I.
- Cerling, T. E., S. J. Morrison, and R. W. Sobocinski (1990), Sediment-water interaction in a small stream: Adsorption of ^{137}Cs by bed loads sediments, *Water Resour. Res.*, 26(6), 1165–1176.
- Cey, E. E., D. L. Rudolph, G. W. Parkin, and R. Aravena (1998), Quantifying groundwater discharge to a small perennial stream in southern Ontario, Canada, *J. Hydrol.*, 210, 21–37, doi:10.1016/S0022-1694(98)00172-3.
- Chen, X. (2004), Streambed hydraulic conductivity for rivers in south-central Nebraska, *J. Am. Water Resour. Assoc.*, 40(3), 561–573, doi:10.1111/j.1752-1688.2004.tb04443.x.
- Chen, X. (2005), Statistical and geostatistical features of streambed hydraulic conductivities in the Platte River, Nebraska, *Environ. Geol.*, 48, 693–701, doi:10.1007/s00254-005-0007-1.
- Chestnut, T. J., and W. H. McDowell (2000), C and N dynamics in the riparian and hyporheic zones of a tropical stream, Luquillo Mountains, Puerto Rico, *J. N. Am. Benthol. Soc.*, 19(2), 199–214, doi:10.2307/1468065.
- Conant, B., Jr. (2004), Delineating and quantifying ground water discharge zones using streambed temperatures, *Ground Water*, 42(2), 243–257, doi:10.1111/j.1745-6584.2004.tb02671.x.
- Conant, B., Jr., J. A. Cherry, and R. W. Gillham (2004), A PCE groundwater plume discharging to a river: Influence of the streambed and near-river zone on contaminant distributions, *J. Contam. Hydrol.*, 73, 249–273, doi:10.1016/j.jconhyd.2004.04.001.
- Craig, A. L. (2005), Evaluation of spatial and temporal variations of groundwater discharge to streams, 121 pp., M.S. thesis, Clemson Univ., Clemson, S. C.
- Duff, J. H., A. J. Tesoriero, and W. B. Richardson (2008), Whole-stream response to nitrate loading in three draining agricultural landscapes, *J. Environ. Qual.*, 37, 1133–1144, doi:10.2134/jeq2007.0187.
- Eaton, A. D., L. S. Clesceri, E. W. Rice, and A. E. Greenberg (2005), Method 4500- NO_3^- I. Cadmium reduction flow injection, and method 4500- NH_3 H. Flow injection analysis, in *Standard Methods for Examination of Water and Wastewater*, edited by A. D. Eaton et al., 21st ed., Am. Public Health Assoc., Washington, D. C.
- Elkins, B. (2007), Nutrient transport between the riparian and hyporheic zones in a small agricultural watershed in the North Carolina Coastal Plain, M.S. thesis, 90 pp., Dep. of Geol. Sci., East Carolina Univ., Greenville, N. C.
- Elliott, A. E., and N. H. Brooks (1997), Transfer of nonsorbing solutes to a streambed with bed forms: Laboratory experiments, *Water Resour. Res.*, 33(1), 137–151, doi:10.1029/96WR02783.
- Fear, J., T. Gallo, N. Hall, J. Loftin, and H. Paerl (2004), Predicting benthic microalgal oxygen and nutrient flux responses to a nutrient reduction management strategy for the eutrophic Neuse River Estuary, NC, USA, *Estuarine Coastal Shelf Sci.*, 61, 491–506, doi:10.1016/j.ecss.2004.06.013.
- Genereux, D. P., S. Leahy, H. Mitasova, C. D. Kennedy, and D. R. Corbett (2008), Spatial and temporal variability of streambed hydraulic conductivity in West Bear Creek, North Carolina, USA, *J. Hydrol.*, 358, 332–353, doi:10.1016/j.jhydrol.2008.06.017.
- Grimm, N. B., and S. G. Fisher (1984), Exchange between interstitial and surface water: Implication for stream metabolism and nutrient cycling, *Hydrobiologia*, 111, 219–228, doi:10.1007/BF00007202.
- Gu, C., G. M. Hornberger, A. L. Mills, J. S. Herman, and S. A. Flewelling (2007), Nitrate reduction in streambed sediments: Effects of flow and biogeochemical kinetics, *Water Resour. Res.*, 43, W12413, doi:10.1029/2007WR006027.
- Gu, C., G. M. Hornberger, J. S. Herman, and A. L. Mills (2008), Influence of stream-groundwater interactions in the streambed sediments on NO_3^- flux to a low-relief coastal stream, *Water Resour. Res.*, 44, W11432, doi:10.1029/2007WR006739.
- Hardy, R. L. (1971), Multiquadratic equations of topography and other irregular surfaces, *J. Geophys. Res.*, 76, 1905–1971, doi:10.1029/JB076i008p01905.
- Hersch, R. W. (1995), *Streamflow Measurement*, 2nd ed., 525 pp., E & FN Spon, London.
- Howarth, R. W., E. W. Boyer, W. J. Pabich, and J. N. Galloway (2002), Nitrogen use in the United States from 1961–2000 and potential future trends, *Ambio*, 31(2), 88–96.
- Jordan, T. E., D. L. Correll, and D. E. Weller (1997), Relating nutrient discharges from watersheds to land use and streamflow variability, *Water Resour. Res.*, 33(11), 2579–2590, doi:10.1029/97WR02005.
- Kennedy, C. D., D. P. Genereux, D. R. Corbett, and H. Mitasova (2007), Design of a light-oil piezomanometer for measurement of hydraulic head differences and collection of groundwater samples, *Water Resour. Res.*, 43, W09501, doi:10.1029/2007WR005904.
- Kennedy, C. D., D. P. Genereux, H. Mitasova, D. R. Corbett, and S. Leahy (2008), Effect of sampling density and design on estimation of streambed attributes, *J. Hydrol.*, 355, 164–180, doi:10.1016/j.jhydrol.2008.03.018.
- Kennedy, C. D., D. P. Genereux, D. R. Corbett, and H. Mitasova (2009), Relationships among groundwater age, denitrification, and the coupled groundwater and nitrogen fluxes through a streambed, *Water Resour. Res.*, 45, W09402, doi:10.1029/2008WR007400.
- Leahy, S. (2007), Spatial and temporal variability in streambed hydraulic conductivity in West Bear Creek, North Carolina, M.S. thesis, 117 pp., Dep. of Mar., Earth, and Atmos. Sci., N. C. State Univ., Raleigh, N. C.
- Lindsey, B. D., S. W. Phillips, C. A. Donnelly, G. K. Speiran, L. N. Plummer, J. K. Böhlke, M. J. Focazio, W. C. Burton, and E. Busenberg (2003), Residence times and nitrate transport in ground water discharging to streams in the Chesapeake Bay watershed, *U.S. Geol. Surv. Water Resour. Invest. Rep.*, 03-4035, 201 pp.
- McCutchan, J. H., Jr., J. F. Saunders III, A. L. Pribyl, and W. M. Lewis Jr. (2003), Open-channel estimation of denitrification, *Limnol. Oceanogr. Methods*, 1, 74–81.
- McMahon, P. B., and J. K. Böhlke (1996), Denitrification and mixing in a stream—Aquifer system: Effects on nitrate loading to surface water, *J. Hydrol.*, 186, 105–128, doi:10.1016/S0022-1694(96)03037-5.
- Merriam, J., W. H. McDowell, and W. S. Curry (1996), A high-temperature catalytic oxidation technique for determining total dissolved nitrogen, *Soil Sci. Soc. Am. J.*, 60, 1050–1055.
- Merwade, V. M., D. R. Maidment, and J. A. Goff (2006), Anisotropic considerations while interpolating river channel bathymetry, *J. Hydrol.*, 331, 731–741, doi:10.1016/j.jhydrol.2006.06.018.
- Mitasova, H., T. G. Drake, R. S. Harmon, and D. Bernstein (2004), Quantifying rapid changes in coastal topography using modern mapping techniques and GIS, *Environ. Eng. Geosci.*, 10(1), 1–11.
- Modica, E., H. T. Buxton, and L. N. Plummer (1998), Evaluating the source and residence time of groundwater seepage to streams, New Jersey Coastal Plain, *Water Resour. Res.*, 34(11), 2797–2810, doi:10.1029/98WR02472.
- Murdoch, L. C., and S. E. Kelly (2003), Factors affecting the performance of conventional seepage meters, *Water Resour. Res.*, 39(6), 1163, doi:10.1029/2002WR001347.
- North Carolina Department of Transportation (2002), US70 (Goldsboro Bypass) from west of SR 1714 to east of SR 1323 in Lenoir county, project: 8.T330802, *Rep. R-2554C*, Raleigh, N. C.
- North Carolina Geological Survey (1985), State geologic map of North Carolina, 1:500,000, Raleigh, N. C.
- Packman, A. I., and K. E. Bencala (2000), Modeling surface-subsurface hydrologic interactions, in *Streams and Ground Waters*, edited by J. B. Jones and P. J. Mulholland, pp. 45–80, Academic, San Diego, Calif.
- Paerl, H. W. (1997), Coastal eutrophication and harmful algal blooms: Importance of atmospheric deposition and groundwater as “new” nitrogen and other nutrient sources, *Limnol. Oceanogr.*, 42(5), 1154–1165.
- Paerl, H. W., J. L. Pinckney, J. M. Fear, and B. J. Peierls (1998), Ecosystem responses to internal and watershed organic matter loading: Consequences for hypoxia in the eutrophying Neuse River Estuary, North Carolina, USA, *Mar. Ecol. Prog. Ser.*, 166, 17–25, doi:10.3354/meps166017.
- Paerl, H. W., L. M. Valdes, M. F. Piehler, and C. A. Stow (2006), Assessing the effects of nutrient management in an estuary experiencing climatic change: The Neuse River Estuary, North Carolina, *Environ. Manage. N. Y.*, 37(3), 422–436, doi:10.1007/s00267-004-0034-9.
- Puckett, L. J. (1995), Identifying the major sources of nutrient water pollution, *Environ. Sci. Technol.*, 29(9), 408A–414A, doi:10.1021/es00009a001.
- Rabalais, N. N., R. E. Turner, and W. J. Wiseman Jr. (2001), Hypoxia in the Gulf of Mexico, *J. Environ. Qual.*, 30, 320–329.
- Reckhow, K., et al. (2004), Designing hydrologic observatories: A paper prototype of the Neuse Watershed, *Tech. Rep. 6*, 84 pp., Consortium of Univ. for the Adv. of Hydrol. Sci., Washington, D. C.
- Sherrell, E. M. (2004), North Carolina Agricultural Statistics 2004, *Publ. 204*, N. C. Dep. of Agric. and Consumer Serv., Raleigh.
- Song, J., X. Chen, C. Cheng, S. Summerside, and F. Wen (2007), Effects of hyporheic processes on streambed vertical hydraulic conductivity in three

- rivers of Nebraska, *Geophys. Res. Lett.*, **34**, L07409, doi:10.1029/2007GL029254.
- Spalding, R. F., and M. E. Exner (1993), Occurrence of nitrate in groundwater: A review, *J. Environ. Qual.*, **22**, 392–394.
- Sprague, L. A., M. J. Langland, S. E. Yochum, R. E. Edwards, J. D. Blomquist, S. W. Phillips, G. W. Shenk, and S. D. Preston (2000), Factors affecting nutrient trends in major rivers of the Chesapeake Bay Watershed, *U.S. Geol. Surv. Water Resour. Invest. Rep.*, 00-4218, 109 pp.
- Springer, J. J., J. M. Burkholder, P. M. Glibert, and R. E. Reed (2005), Use of a real-time remote monitoring network and shipborne sampling to characterize a dinoflagellate bloom in the Neuse Estuary, North Carolina, U.S.A., *Harmful Algae*, **4**, 533–551, doi:10.1016/j.hal.2004.08.017.
- Spruill, T. B., A. J. Tesoriero, H. E. Mew Jr., K. M. Farrell, S. L. Harden, A. B. Colosimo, and S. R. Kraemer (2005), Geochemistry and characteristics of nitrogen transport at a confined animal feeding operation in a coastal plain agricultural watershed, and implications for nutrient loading in the Neuse River Basin, North Carolina, 1999–2002, *U.S. Geol. Surv. Sci. Invest. Rep.*, 2004-5283, 57 pp.
- Staver, K. W., and R. B. Brinsfield (1996), Seepage of groundwater nitrate from a riparian agroecosystem into the Wye River estuary, *Estuaries Coasts*, **19**(2), 359–370.
- Stow, C. A., M. E. Borsuk, and K. H. Reckhow (2007), Ecosystem risk assessment: A case study of the Neuse River Estuary, in *Risk Assessment for Environmental Health*, edited by M. Robson and W. Toscano, pp. 563–585, Jossey Bass, San Francisco, Calif.
- Tesoriero, A. J., H. Liebscher, and S. E. Cox (2000), Mechanism and rate of denitrification in an agricultural watershed: Electron and mass balance along groundwater flow paths, *Water Resour. Res.*, **36**(6), 1545–1559, doi:10.1029/2000WR900035.
- Tesoriero, A. J., T. B. Spruill, H. E. Mew Jr., K. M. Farrell, and S. K. Harden (2005), Nitrogen transport and transformations in a coastal plain watershed: Influence of geomorphology on flow paths and residence times, *Water Resour. Res.*, **41**, W02008, doi:10.1029/2003WR002953.
- Tesoriero, A. J., D. A. Saad, K. R. Burow, E. A. Frick, L. J. Puckett, and J. E. Barbash (2007), Linking ground water age and chemistry data along flow paths: Implications for trends and transformations of nutrients and pesticides, *J. Contam. Hydrol.*, **94**, 139–155, doi:10.1016/j.jconhyd.2007.05.007.
- Thibodeaux, L. J., and J. D. Boyle (1987), Bedform-generated convective transport in bottom sediment, *Nature*, **325**, 341–343, doi:10.1038/325341a0.
- Tiedje, J. M. (1988), Ecology of denitrification and dissimilatory nitrate reduction to ammonium, in *Biology of Anaerobic Microorganisms*, edited by A. J. B. Zehnder, pp. 179–244, John Wiley, New York.
- U.S. Environmental Protection Agency and U.S. Department of Agriculture (1993), Determination of inorganic anions by ion chromatography, U.S. Environmental Protection Agency method 300.0, revision 2.1, Cincinnati, Ohio.
- U.S. Environmental Protection Agency (USEPA) (1994), Methods from determination of metals in environmental samples—Supplement 1, *Rep. EPA-600/R-94-11*, Washington, D. C.
- U.S. Environmental Protection Agency (USEPA) (1998), Clean water action plan: Restoring and protecting America's water, 28 pp., Washington, D. C.
- Usry, B. P. (2005), Nitrogen loading in the Neuse River basin, North Carolina: The RIVERNET monitoring program, M.S. thesis, 105 pp., Dep. of Mar., Earth, and Atmos. Sci., N. C. State Univ., Raleigh.
- Valett, H. M., S. G. Fisher, N. B. Grimm, and P. Camill (1994), Vertical hydrologic exchange and ecological stability of a desert stream ecosystem, *Ecology*, **75**(2), 548–560, doi:10.2307/1939557.
- Winner, M. D., Jr., and R. W. Coble (1996), Hydrogeologic framework of the North Carolina Coastal Plain, *U.S. Geol. Surv. Prof. Pap.*, 1404-I, 106 pp.
- Zar, J. H. (1999), *Biostatistical Analysis*, 4th ed., 663 pp., Prentice Hall, Upper Saddle River, N. J.

D. R. Corbett, Department of Geological Sciences, East Carolina University, Greenville, NC 27858, USA.

D. P. Genereux and H. Mitasova, Department of Marine, Earth, and Atmospheric Sciences, North Carolina State University, Campus Box 8208, Raleigh, NC 27695-8208, USA.

C. D. Kennedy, Department of Earth and Atmospheric Sciences, Purdue University, 550 Stadium Mall Drive, West Lafayette, IN 47907-2051, USA. (cdkennedy@purdue.edu)